

SUPPORTING INFORMATION

**Novel Paraben Derivatives of Tetracyclic  
Spermine Cyclotriphosphazenes: Synthesis,  
Characterization and Biosensor based DNA  
Interaction Analysis**

*Perihan Kızılkaya<sup>1,2</sup>, Elif Şenkuytu<sup>1,3\*</sup>, Derya Davarçı<sup>1</sup>, Uğur Pala<sup>1</sup>, Zehra Ölçer<sup>1</sup> and Gönül*

*Yenilmez Çiftçi<sup>1</sup>*

<sup>1</sup>Department of Chemistry, Gebze Technical University, Gebze, Kocaeli, Turkey

<sup>2</sup>Faculty of Arts and Science, Department of Chemistry, Trakya University, Edirne, Turkey

<sup>3</sup>Faculty of Science, Department of Chemistry, Atatürk University, Erzurum, Turkey

\*Corresponding author: Dr. Elif Şenkuytu,  
e-mail:[elif.senkuytu@atauni.edu.tr](mailto:elif.senkuytu@atauni.edu.tr); Tel: +90 4422314114

## TABLE OF CONTENTS

<b>EXPERIMENTAL SECTION</b> .....	2
<b>Figure S1:</b> Mass spectrum of compound <b>1</b> .....	7
<b>Figure S2:</b> <sup>1</sup> H NMR spectrum of compound <b>1</b> .....	7
<b>Figure S3:</b> <sup>1</sup> H NMR spectrum of compound <b>1</b> after D <sub>2</sub> O exchange.....	8
<b>Figure S4:</b> The proton decoupled <sup>31</sup> P NMR spectrum of the compound <b>1</b> .....	8
<b>Figure S5:</b> The proton coupled <sup>31</sup> P NMR spectrum of the compound <b>1</b> .....	9
<b>Figure S6:</b> Mass spectrum of compound <b>2</b> .....	9
<b>Figure S7:</b> <sup>1</sup> H NMR spectrum of compound <b>2</b> .....	10
<b>Figure S8:</b> <sup>1</sup> H NMR spectrum of compound <b>2</b> after D <sub>2</sub> O exchange.....	10
<b>Figure S9:</b> The proton decoupled <sup>31</sup> P NMR spectrum of the compound <b>2</b> .....	11
<b>Figure S10:</b> The proton coupled <sup>31</sup> P NMR spectrum of the compound <b>2</b> .....	11
<b>Figure S11:</b> Mass spectrum of compound <b>3</b> .....	12
<b>Figure S12:</b> <sup>1</sup> H NMR spectrum of compound <b>3</b> .....	12
<b>Figure S13:</b> <sup>1</sup> H NMR spectrum of compound <b>3</b> after D <sub>2</sub> O exchange.....	13
<b>Figure S14:</b> The proton decoupled <sup>31</sup> P NMR spectrum of the compound <b>3</b> .....	13
<b>Figure S15:</b> The proton coupled <sup>31</sup> P NMR spectrum of the compound <b>3</b> .....	14
<b>Figure S16:</b> Mass spectrum of compound <b>4</b> .....	14
<b>Figure S17:</b> <sup>1</sup> H NMR spectrum of compound <b>4</b> .....	15
<b>Figure S18:</b> <sup>1</sup> H NMR spectrum of compound <b>4</b> after D <sub>2</sub> O exchange.....	15
<b>Figure S19:</b> The proton decoupled <sup>31</sup> P NMR spectrum of the compound <b>4</b> .....	16
<b>Figure S20:</b> The proton coupled <sup>31</sup> P NMR spectrum of the compound <b>4</b> .....	16
<b>Figure S21:</b> Mass spectrum of compound <b>5</b> .....	17
<b>Figure S22:</b> <sup>1</sup> H NMR spectrum of compound <b>5</b> .....	17
<b>Figure S23:</b> <sup>1</sup> H NMR spectrum of compound <b>5</b> after D <sub>2</sub> O exchange.....	18
<b>Figure S24:</b> The proton decoupled <sup>31</sup> P NMR spectrum of the compound <b>5</b> .....	18
<b>Figure S25:</b> The proton coupled <sup>31</sup> P NMR spectrum of the compound <b>5</b> .....	19
<b>Figure S26:</b> Mass spectrum of compound <b>6</b> .....	19
<b>Figure S27:</b> <sup>1</sup> H NMR spectrum of compound <b>6</b> .....	20
<b>Figure S28:</b> <sup>1</sup> H NMR spectrum of compound <b>6</b> after D <sub>2</sub> O exchange.....	20
<b>Figure S29:</b> The proton decoupled <sup>31</sup> P NMR spectrum of the compound <b>6</b> .....	21
<b>Figure S30:</b> The proton coupled <sup>31</sup> P NMR spectrum of the compound <b>6</b> .....	21
<b>Figure S31:</b> DSC curves of compounds <b>2</b> , <b>4</b> and <b>5</b> .....	22
<b>Table S1.</b> Selected bond lengths and bond angles of compounds <b>2</b> , <b>4</b> and <b>5</b> .....	23
<b>Table S2.</b> Selected conformational parameters of <b>2</b> , <b>3</b> and <b>5</b> .....	24
<b>Table S3.</b> X-H...π interactions for <b>2</b> , <b>4</b> and <b>5</b> .....	24
<b>Table S4.</b> Hydrogen bond parameters (Å and °) for <b>2</b> , <b>4</b> and <b>5</b> .....	24
<b>Figure S32:</b> Fully integrated and b automated biosensor device (a-b-c) and its biochip (d).....	25
<b>Figure S33:</b> The cyclic voltammetry using bare and MUDA coated gold electrode arrays (1 mM K <sub>4</sub> [Fe(CN) <sub>6</sub> ]/KCl at 100 mV/s scan rate).....	25
<b>Figure S34:</b> The amperometric responses were shown as percent relative hybridization responses in the figure, percentages of interacting DNA are shown (Compounds at 0, 12.5, 25 and 50 μM concentrations were incubated with DNA probes before injection onto the biochip) .....	26
<b>Figure S35:</b> The amperometric responses were shown as percent relative hybridization responses in the figure, indicated by remaining from interaction DNA of Parabens (0, 12.5, 25 and 50 μM) were incubated with DNA probes prior to the injection on to the biochip.....	27
<b>Figure S36:</b> Agarose gel images of pUC18 plasmid DNA when incubated with different concentrations of compound <b>1</b> .....	27
<b>Figure S37:</b> Agarose gel images of pUC18 plasmid DNA when incubated with different concentrations of compound <b>2</b> .....	28
<b>Figure S38:</b> Agarose gel images of pUC18 plasmid DNA when incubated with different concentrations of compound <b>3</b> .....	28
<b>Figure S39:</b> Agarose gel images of pUC18 plasmid DNA when incubated with different concentrations of compound <b>4</b> .....	29
<b>Figure S40:</b> Agarose gel images of pUC18 plasmid DNA when incubated with different concentrations of compound <b>5</b> .....	29
<b>Figure S41:</b> Agarose gel images of pUC18 plasmid DNA when incubated with different concentrations of compound <b>6</b> .....	30

## EXPERIMENTAL SECTION

### 1. General chemical material and methods

Hexachlorocyclotriphosphazene (trimer) (Otsuka Chemical Co., Ltd) was purified by fractional crystallization from n-hexane. Sodium hydride, (60% dispersion in mineral oil, Merck; prior to use the oil was removed by washing with dry heptane followed by decantation). Methyl 4-hydroxybenzoate (99.0%), ethyl 4-hydroxybenzoate (99.0%), n-propyl 4-hydroxybenzoate (99.0%), n-butyl 4-hydroxybenzoate (99.0%) were obtained from Alfa Aesar, benzyl 4-hydroxybenzoate (99.0%) was obtained from Aldrich and Spermine (99.0%) was obtained from Sigma. Tetrahydrofuran (99.0%), dichloromethane (99.0%), n-hexane (95.0%) were obtained from Merck. Silica gel 60 (230–400 mesh) for column chromatography was obtained from Merck. CDCl<sub>3</sub> for NMR spectroscopy was obtained from Goss Scientific.

Positive ion and linear mode MALDI-MS of compounds were obtained in dithranol as MALDI matrix using nitrogen laser accumulating 50 laser shots using Bruker Microflex LT MALDI-TOF mass spectrometer. All reagents were purchased from Aldrich and used without further purification and all solvents were obtained from Merck. All reactions were monitored by thin layer chromatography using Merck TLC Silica gel 60 F<sub>254</sub>. Silica gel 60 (particle size: 0.040-0.063 mm, 230-400 mesh ASTM) for column chromatography was obtained from Merck. All reactions were carried out under an argon atmosphere. <sup>1</sup>H and <sup>31</sup>P NMR spectra were recorded for all compounds in CDCl<sub>3</sub> solutions on a Varian INOVA 500 MHz spectrometer. Thermal stabilities of the compounds were investigated by Mettler Toledo TGA/SDTA 851 thermogravimetric analyses (TGA) and melting points were measured by differential scanning calorimeter DSC 821<sup>o</sup> (DSC) equipped with Mettler Toledo Star<sup>c</sup> software at a heating rate of 10 °C min<sup>-1</sup> under spectroscopic grade argon flow (50 mL min<sup>-1</sup>) between 25 and 700 °C for TGA and 25 to 300 °C for DSC, respectively. DNA interaction analysis tests were performed using an automated biosensor device and its sensor chips (BILGEM-TUBITAK, Kocaeli, Turkey).

### 2. Biosensor device and DNA interaction tests

Phosphate buffered saline tablets, mercaptoundecanoic acid, ethanolamine, horseradish peroxidase (HRP), 3,3',5,5'-Tetramethylbenzidine (TMB) ready to use reagent, hydrochloric acid (HCl), Tris-HCl, N-hydroxysuccinimide (NHS) were purchased from Sigma-Aldrich. 1-ethyl-3-(3-dimethylaminopropyl)-carbodiimide (EDC) and NeutrAvidin (NA) was purchased from Thermo Scientific. Au nanoparticles (15nm) were obtained from BBI International. The oligonucleotide sequences were obtained from TIB Molbiol (Oligonucleotide Sequences).

#### HPLC Purified Oligonucleotides:

***Target probe:*** 5'- AGA CGT TAA TAC ATT GAA CCT GTT TTC CGA CCC ATT C -3'  
Molecular Weight (g/mol), 11911.6

**Surface probe:** Biotin - CAA TAT TTG GCG T GA ATG GGT CGG AAA ACA  
Molecular Weight (g/mol), 9813.1

**Detection probe:** 5'- GGT TCA ATG TAT TAA CGT CTA TGG AAA – Biotin  
Molecular Weight (g/mol), 8780.3

### 3. X-ray data collection and structure refinement

Suitable single crystals of **2**, **4** and **5** were carefully separated from other crystals in the crystallization vessel under a polarizing microscope and placed on a thin glass fibre using perfluoropolyether oil. The solid-state structures of the complexes were confirmed by X-ray crystallography. Data were obtained on a Bruker APEX II QUAZAR three-circle diffractometer using monochromatized Mo K $\alpha$  X-radiation ( $\lambda = 0.71073 \text{ \AA}$ ). Indexing was performed using APEX2 [2]. Data integration and reduction were carried out with SAINT [3]. Absorption correction was performed by multi-scan method implemented in SADABS [4]. The structure was solved using SHELXT [5] and then refined by full-matrix least-squares refinements on  $F^2$  using the SHELXL [6] in OLEX 2 program package [7]. All non-hydrogen atoms were refined anisotropically using all reflections with  $I > 2\sigma(I)$ . The positions of the N-bound H atoms were located according to the calculated positions. Aromatic and aliphatic C-bound H atoms were positioned geometrically and refined using a riding mode. Crystallographic data and refinement details of the data collection for the compounds were given in Table 2 in manuscript. Crystal structure validations and geometrical calculations were performed using Platon software [8]. Mercury software [9] was used for visualization of the cif files. Additional crystallographic data with CCDC reference numbers 2009792 for **2**; 2009793 for **4**; 2009794 for **5** have been deposited within the Cambridge Crystallographic Data Center via [www.ccdc.cam.ac.uk/deposit](http://www.ccdc.cam.ac.uk/deposit).

[2] Bruker (2007) APEX2, Bruker AXS Inc., Madison, Wisconsin, USA.

[3] Bruker (2007) SAINT, Bruker AXS Inc., Madison, Wisconsin, USA.

[4] Bruker (2001) SADABS, Bruker AXS Inc., Madison, Wisconsin, USA.

[5] G. M. Sheldrick, Acta Cryst., A71 (2015) 3-8

[6] G. M. Sheldrick, Acta Cryst., C71, (2015) 3-8.

[7] O.V. Dolomanov, L.J. Bourhis, R.J. Gildea, J.A.K. Howard, H. Puschmann, J. Appl. Cryst., 42 (2009) 339-341

[8] A. L. Spek, Acta Cryst. D65 (2009) 148-155.

[9] C. F. Macrae, P. R. Edgington, P. McCabe, E. Pidcock, G. P. Shields, R. Taylor, M. Towler, J. van de Streek, J. Appl. Cryst., 39 (2006) 453-457.

### 4. Synthesis

**Synthesis of compound 1.** Compound **1** was synthesized according to literature [10] and spectral data of compound **1** was given in Figure S1-S5.

[10] T. S. Cameron, A. Linden, G. Guerch, J. P. Bonnet and J. F. Labarre, *J. Mol. Struct.*, 1989, **212**, 295-304.

**Synthesis of compound 2.** Methyl 4-hydroxybenzoate, (0.79 g, 5.19 mmol) and NaH (0.21 g, 5.19 mmol) were dissolved in 30 mL of dry THF under an argon atmosphere in a 100 mL three-necked round-bottomed flask. The reaction mixture was cooled in an ice-bath and compound **1** (1.00 g, 2.47 mmol) in 20 mL of dry THF was added dropwise over 30 minutes to a stirred solution under an argon atmosphere. The reaction mixture was refluxed in an oil bath with stirring for 5 days and followed on TLC silica gel plates using *n*-hexane: THF (3:4) as eluant. The reaction mixture was filtered to remove the sodium chloride formed and the solvent removed under reduced pressure. The resulting white solid was subjected to column chromatography using *n*-hexane–THF (3:4) as eluant. Compound **2**, isolated as white solid (1.17 g, 1.8 mmol, 75%, mp: 166.33 °C). Compound **2** was re-crystallized from *n*-hexane: THF (4:3) and obtained as white crystals, which were suitable for single crystal X-ray crystallography.

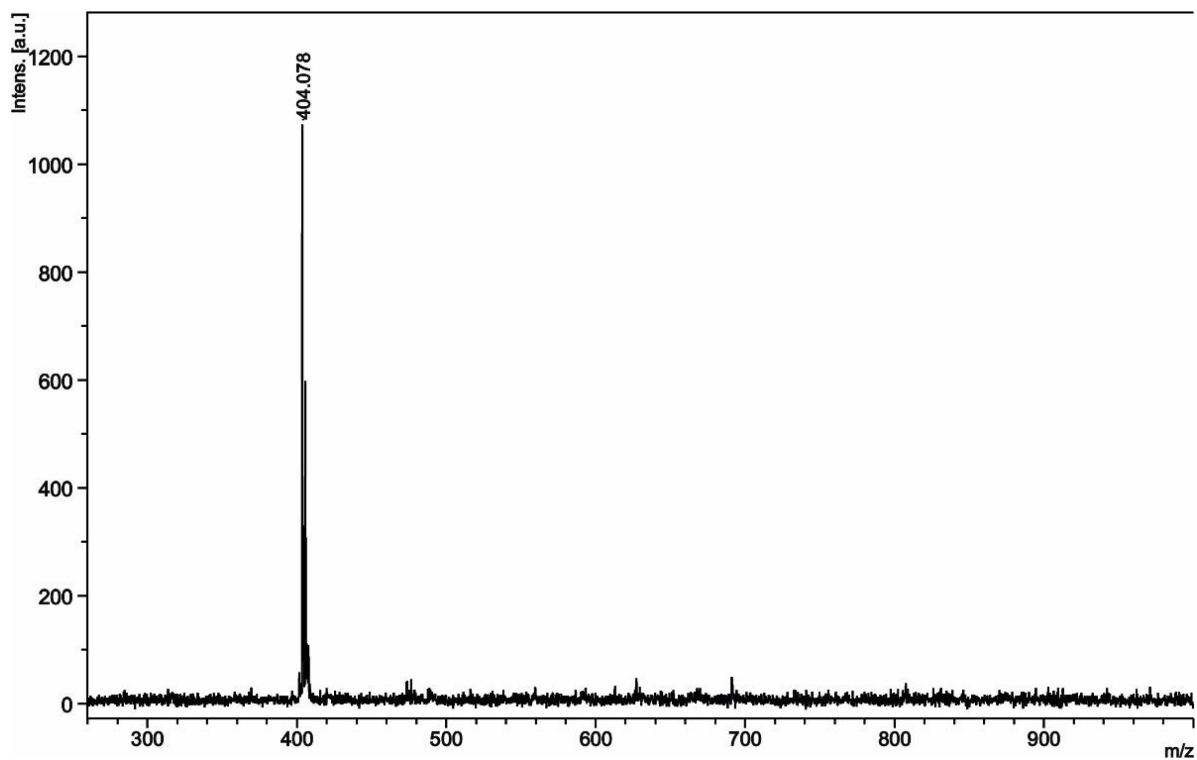
**Synthesis of compound 3.** Ethyl 4-hydroxybenzoate, (0.86 g, 5.19 mmol) and NaH (0.21 g, 5.19 mmol) were dissolved in 30 mL of dry THF under an argon atmosphere in a 100 mL three-necked round-bottomed flask. The reaction mixture was cooled in an ice-bath and compound **1** (1.00 g, 2.47 mmol) in 20 mL of dry THF was added dropwise over 30 minutes to a stirred solution under an argon atmosphere. The reaction mixture was refluxed in an oil bath with stirring for 5 days and followed on TLC silica gel plates using *n*-hexane: THF (2:3) as eluant. The reaction mixture was filtered to remove the sodium chloride formed and the solvent removed under reduced pressure. The resulting white solid was subjected to column chromatography using *n*-hexane: THF (2:3) as eluant. Compound **3**, isolated as oily (1.18 g, 1.7 mmol, 72%, oily).

**Synthesis of compound 4.** Propyl 4-hydroxybenzoate, (0.86 g, 5.19 mmol) and NaH (0.21 g, 10.64 mmol) were dissolved in 30 mL of dry THF under an argon atmosphere in a 100 mL three-necked round-bottomed flask. The reaction mixture was cooled in an ice-bath and compound **1** (1.00 g, 2.47 mmol) in 20 mL of dry THF was added dropwise over 30 minutes to a stirred solution under an argon atmosphere. The reaction mixture was refluxed in an oil bath with stirring for 5 days and followed on TLC silica gel plates using *n*-hexane: THF (3:4) as eluant. The reaction mixture was filtered to remove the sodium chloride formed and the solvent removed under reduced pressure. The resulting white solid was subjected to column chromatography using *n*-hexane: THF (3:4) as eluant. Compound **4**, isolated as white solid (1.47 g, 2.12 mmol, 86%, mp: 131.36 °C). Compound **4** was re-crystallized from *n*-hexane: THF (3:4) and obtained as white crystals, which were suitable for single crystal X-ray crystallography.

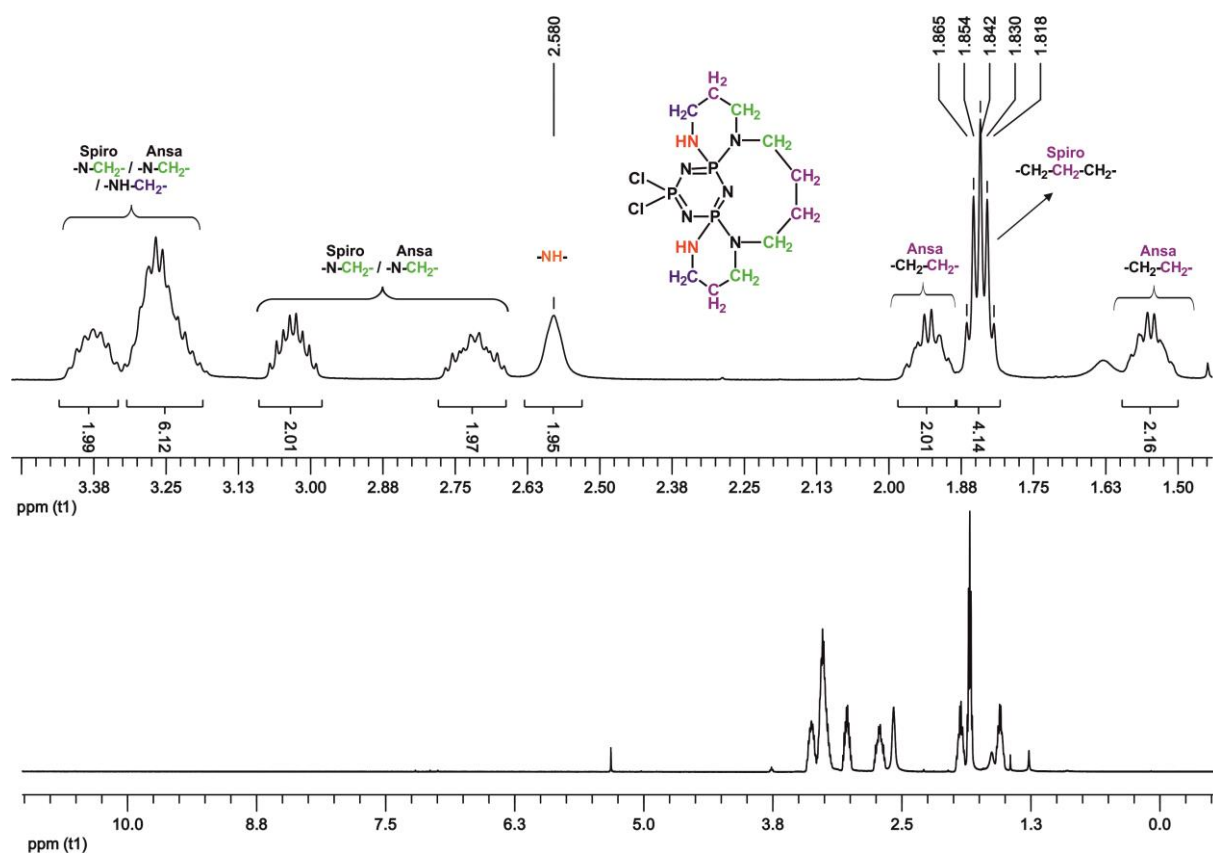
**Synthesis of compound 5.** Butyl 4-hydroxybenzoate, (1.01 g, 5.19 mmol) and NaH (0.21 g, 5.19 mmol) were dissolved in 30 mL of dry THF under an argon atmosphere in a 100 mL three-necked round-bottomed flask. The reaction mixture was cooled in an ice-bath and compound **1** (1.00 g, 2.47 mmol) in 20 mL of dry THF was added dropwise over 30 minutes to a stirred solution under an argon atmosphere. The reaction mixture was refluxed in an oil bath with stirring for 5 days and followed on TLC silica gel plates using *n*-hexane: THF (3:4)

as eluant. The reaction mixture was filtered to remove the sodium chloride formed and the solvent removed under reduced pressure. The resulting white solid was subjected to column chromatography using *n*-hexane: THF (3:4) as eluant. Compound **5**, isolated as white solid (1.51 g, 2.1 mmol, 85%, 95.11 °C). Compound **5** was re-crystallized from *n*-hexane: THF (3:4) and obtained as white crystals, which were suitable for single crystal X-ray crystallography.

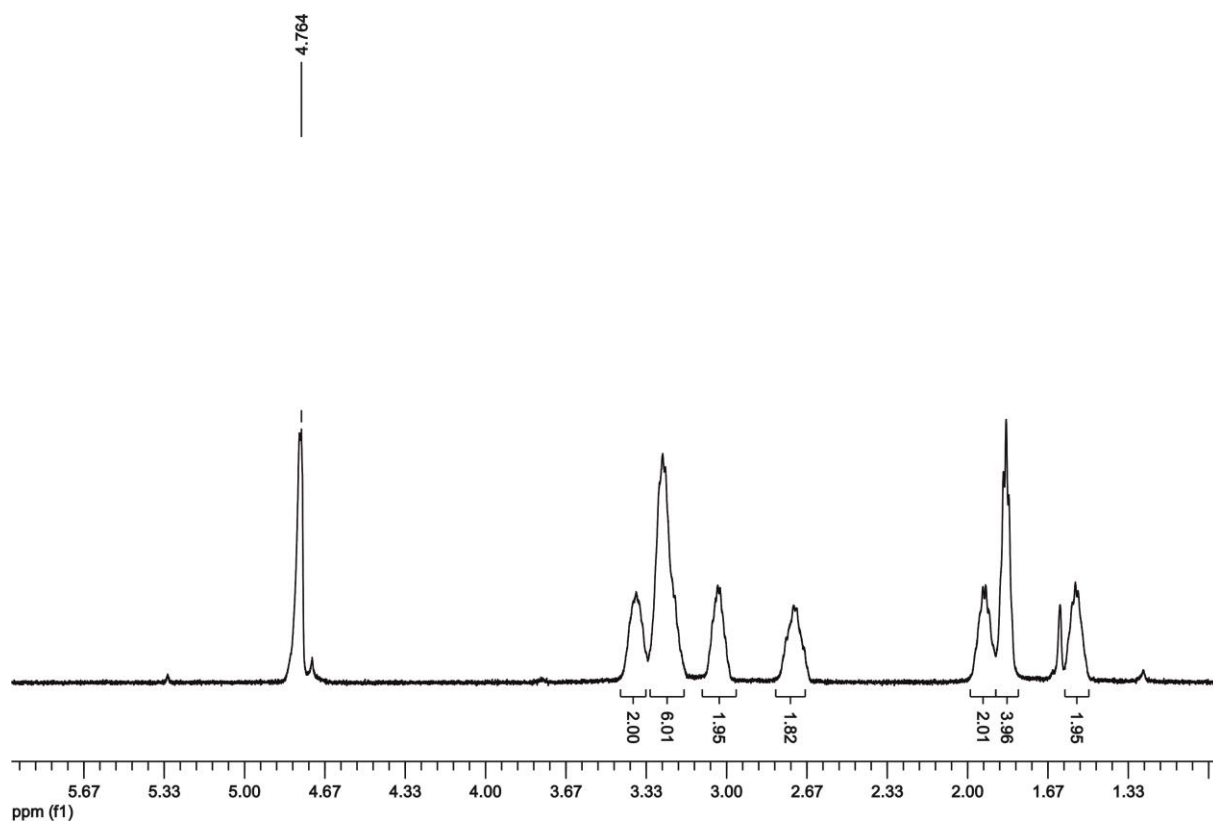
**Synthesis of compound 6.** Benzyl 4-hydroxybenzoate, (1.18 g, 5.19 mmol) and NaH (0.21 g, 5.19 mmol) were dissolved in 30 mL of dry THF under an argon atmosphere in a 100 mL three-necked round-bottomed flask. The reaction mixture was cooled in an ice-bath and compound **1** (1.00 g, 2.47 mmol) in 20 mL of dry THF was added dropwise over 30 minutes to a stirred solution under an argon atmosphere. The reaction mixture was refluxed in an oil bath with stirring for 5 days and followed on TLC silica gel plates using *n*-hexane: THF (3:4) as eluant. The reaction mixture was filtered to remove the sodium chloride formed and the solvent removed under reduced pressure. The resulting white solid was subjected to column chromatography using *n*-hexane: THF (3:4) as eluant. Compound **6**, isolated as oily (1.73 g, 2.2 mmol, 89%, oily).



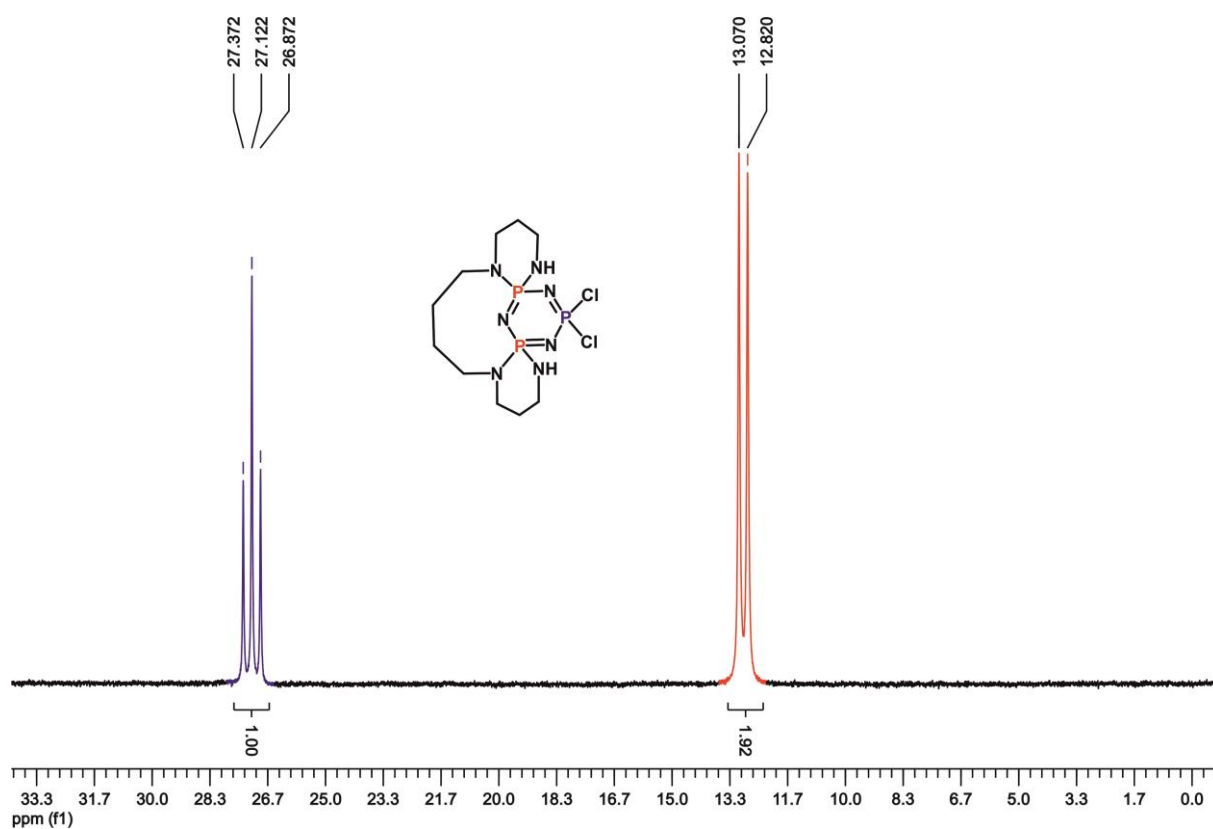
**Figure S1:** Mass spectrum of compound **1**



**Figure S2:** <sup>1</sup>H NMR spectrum of compound **1**

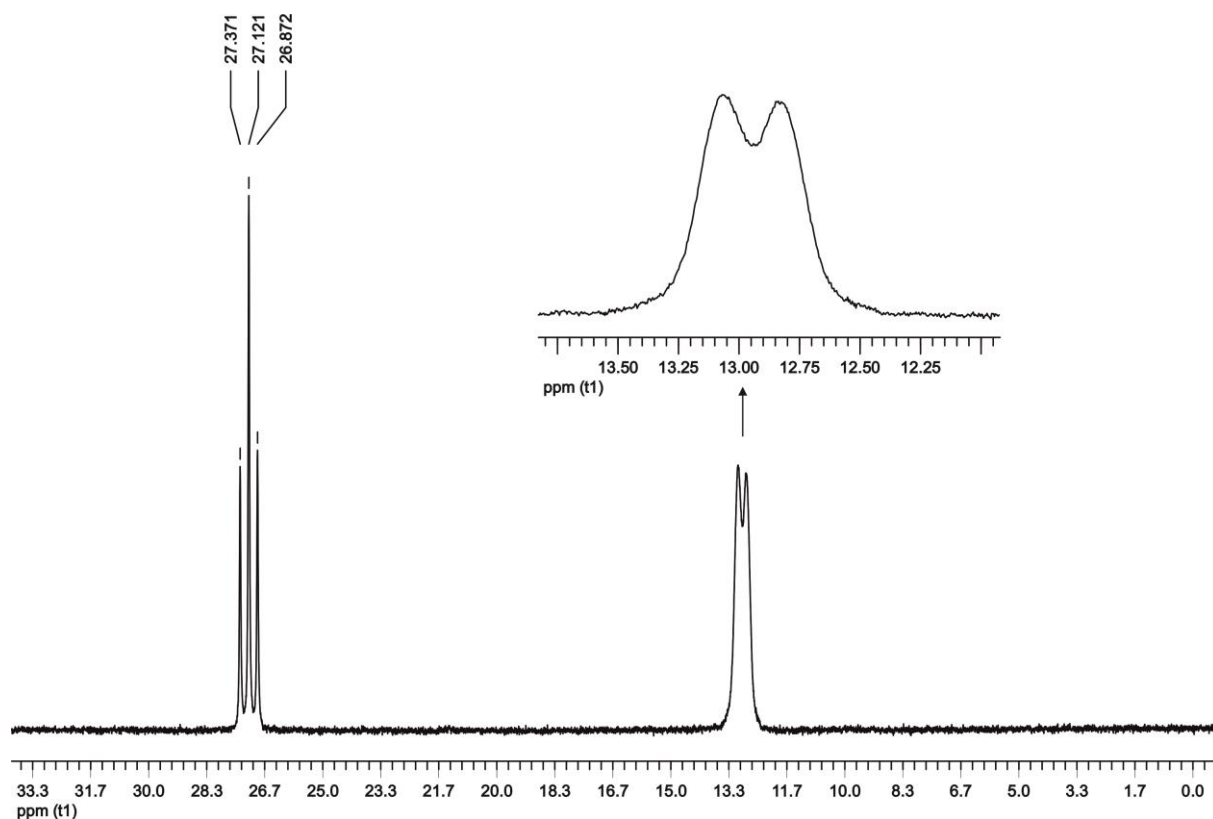


**Figure S3:**  $^1\text{H}$  NMR spectrum of compound **1** after  $\text{D}_2\text{O}$  exchange

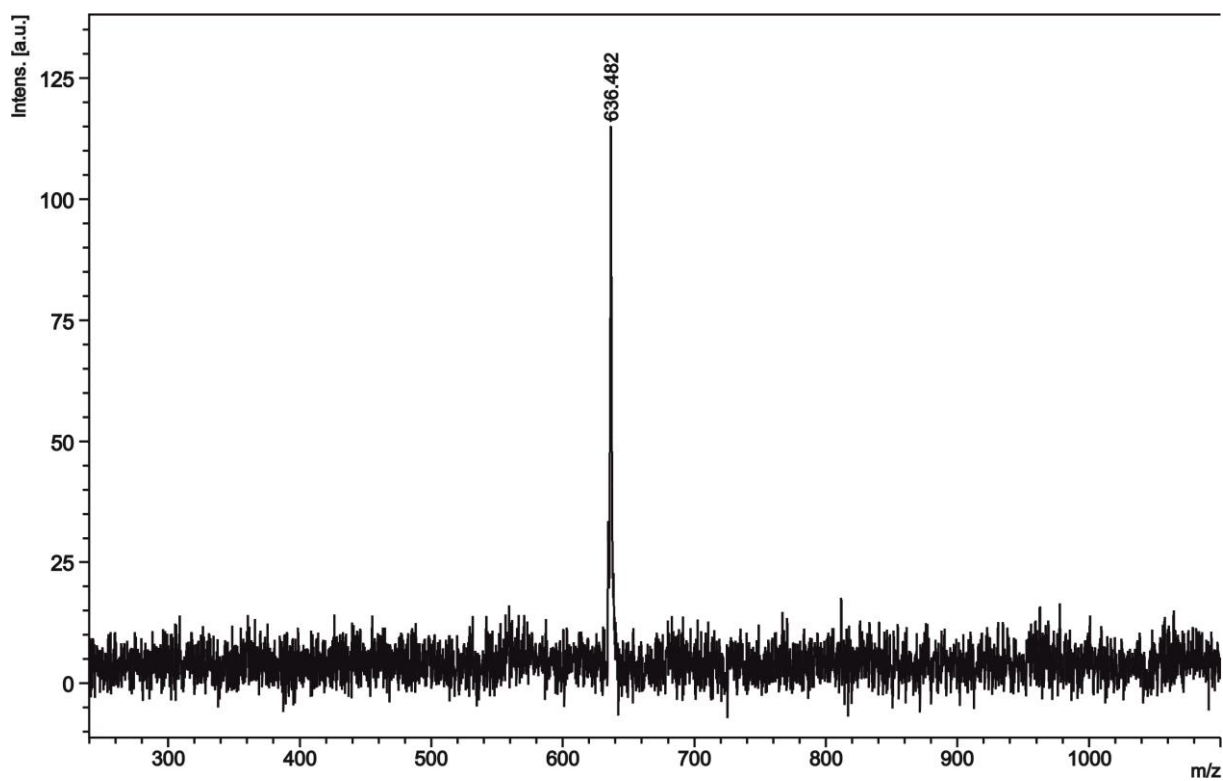


**Figure S4:** The proton decoupled  $^{31}\text{P}$  NMR spectrum of the compound **1**

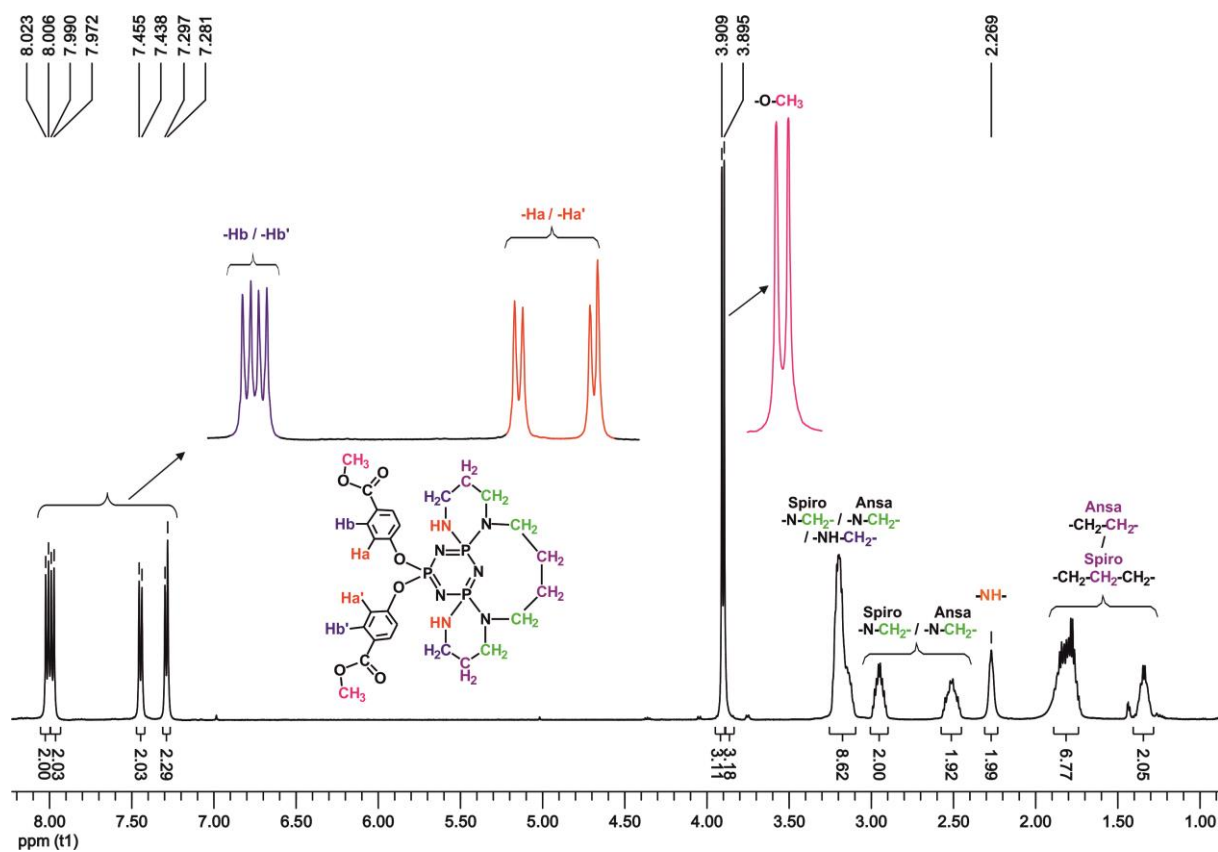




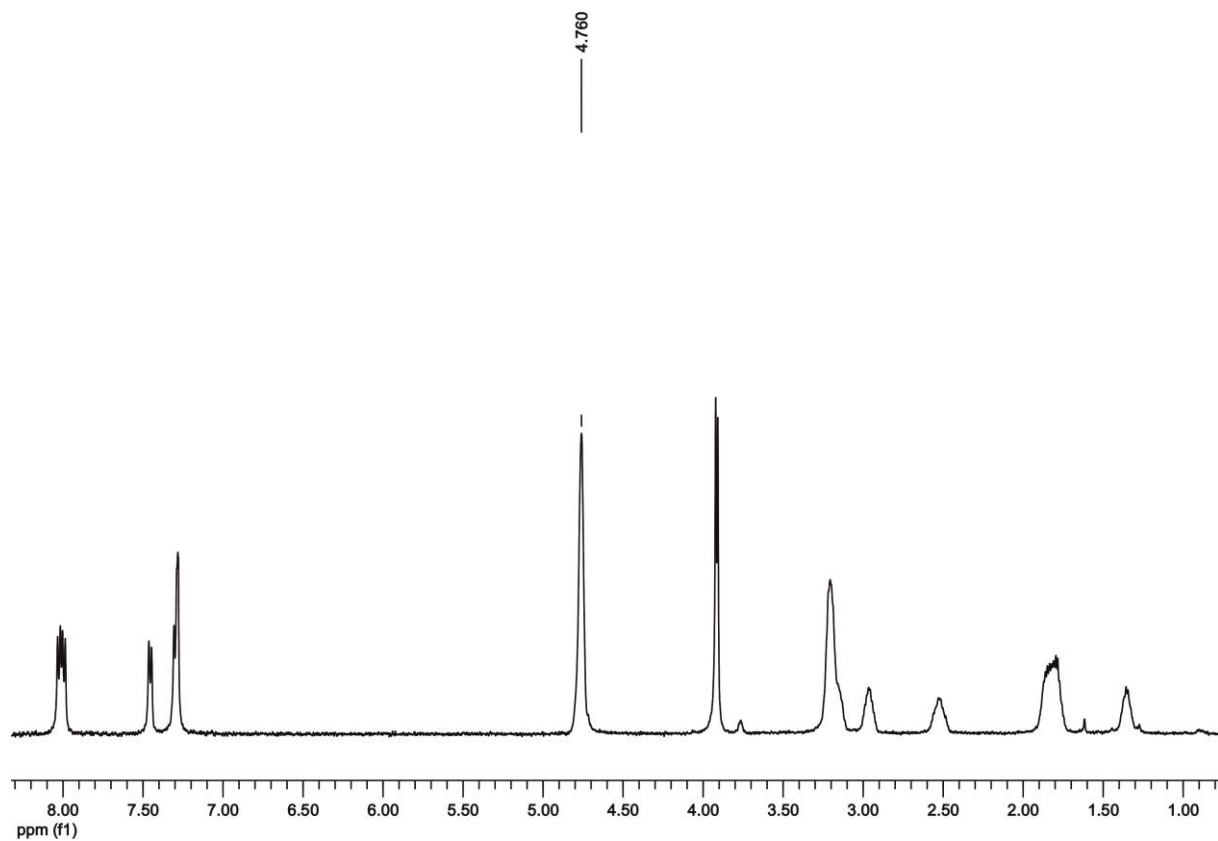
**Figure S5:** The proton coupled  $^{31}\text{P}$  NMR spectrum of the compound **1**



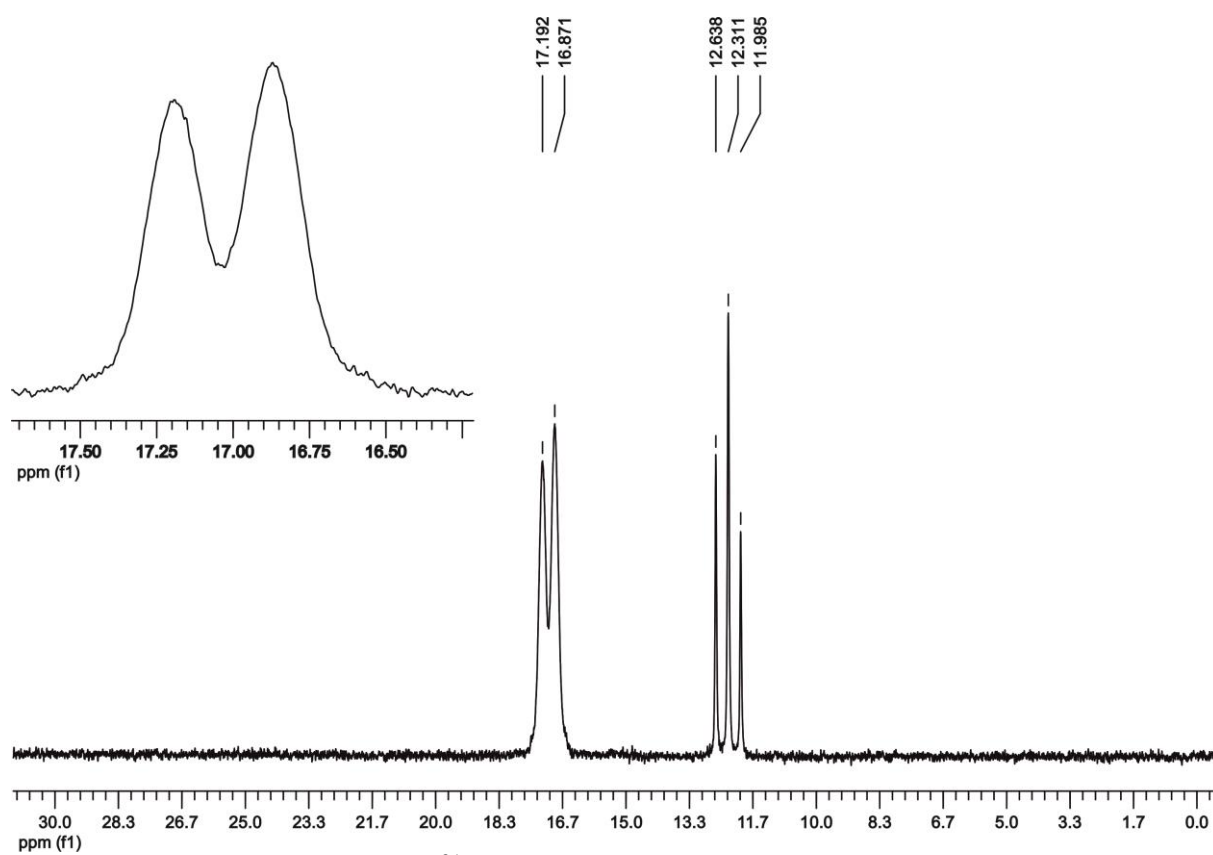
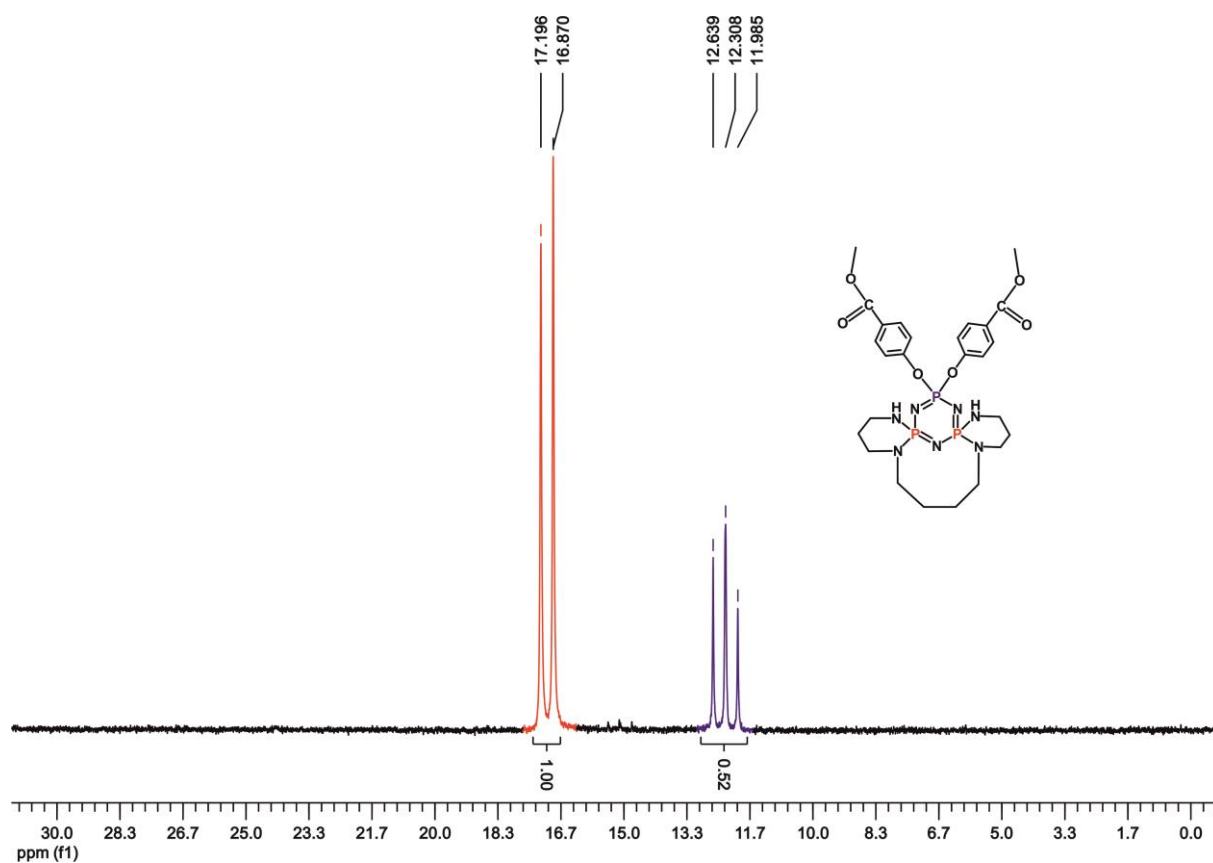
**Figure S6:** Mass spectrum of compound **2**



**Figure S7:** <sup>1</sup>H NMR spectrum of compound 2



**Figure S8:** <sup>1</sup>H NMR spectrum of compound 2 after D<sub>2</sub>O exchange



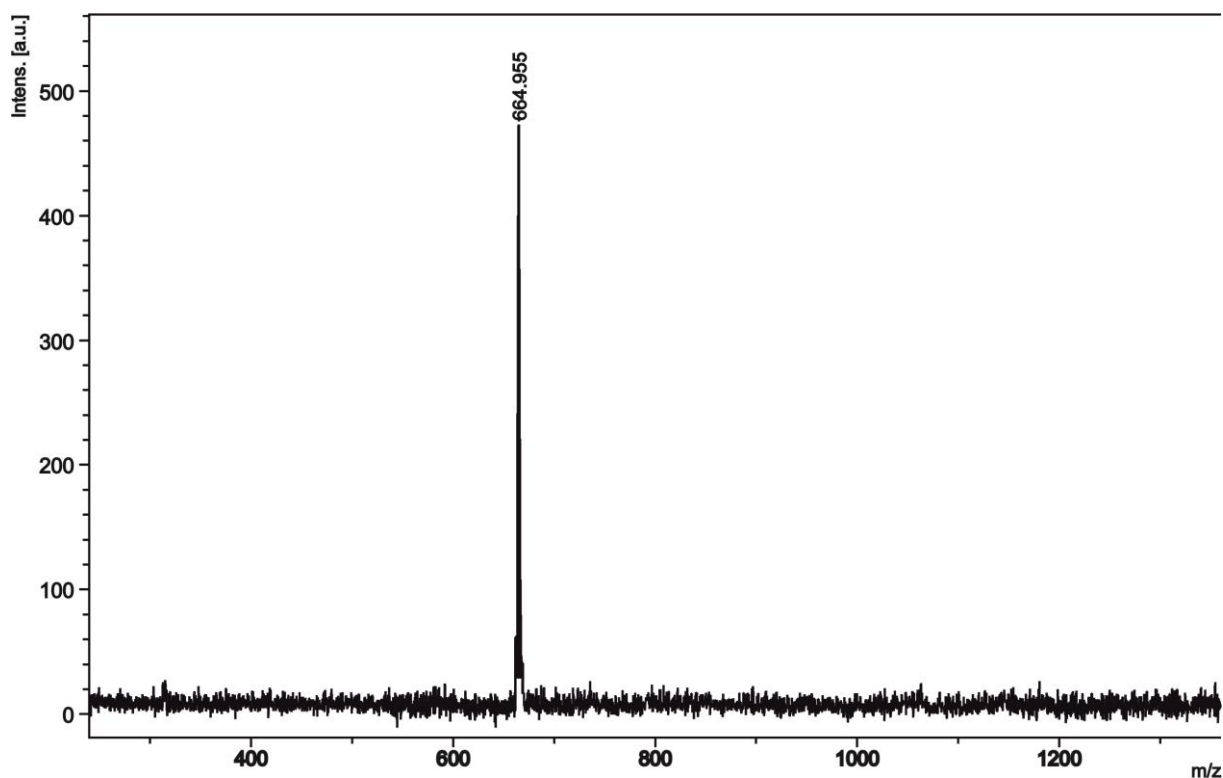


Figure S11: Mass spectrum of compound 3

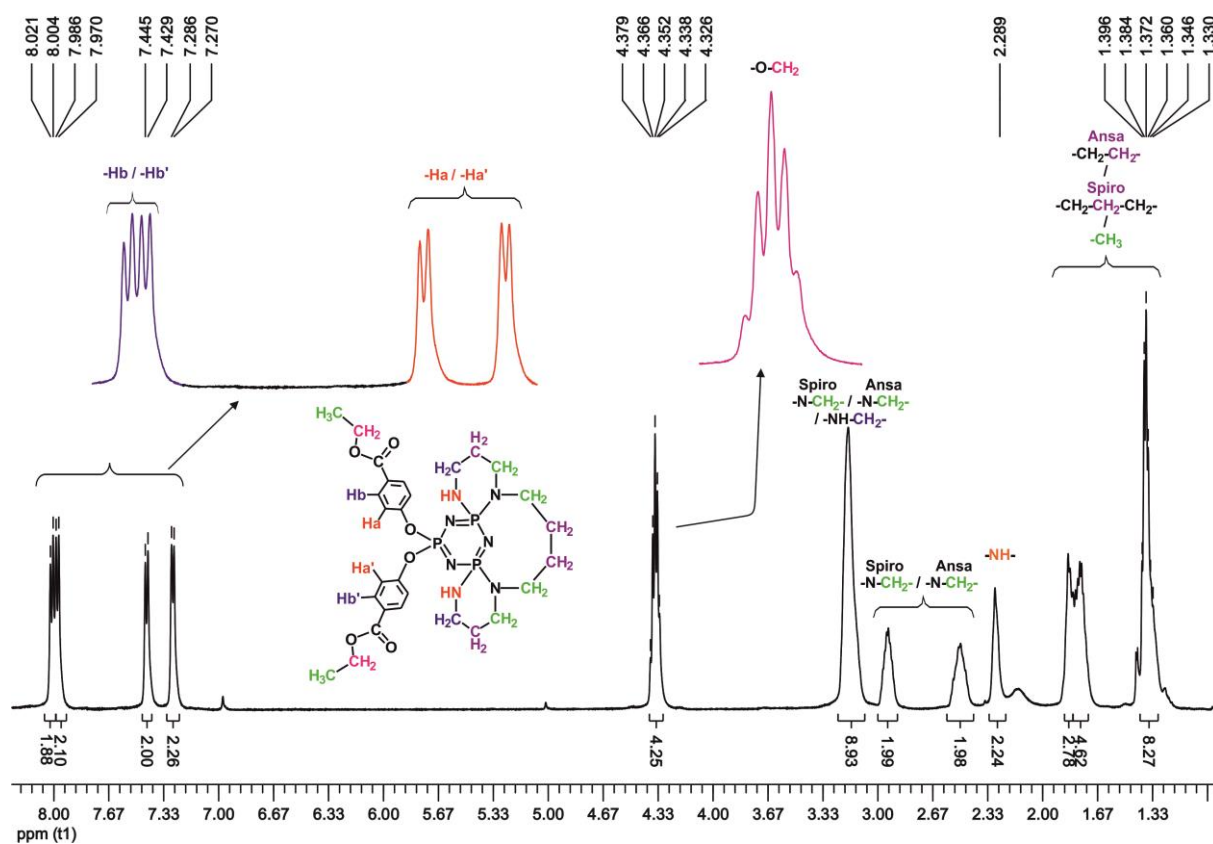
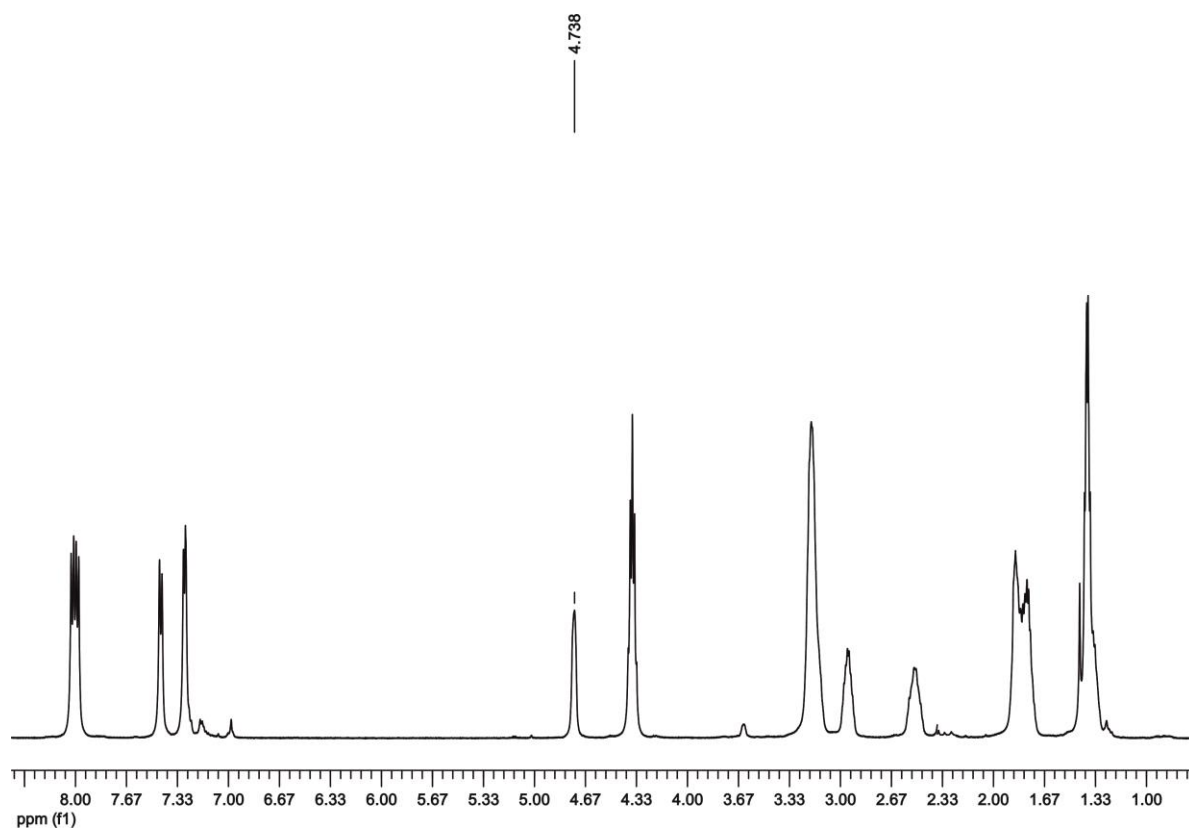
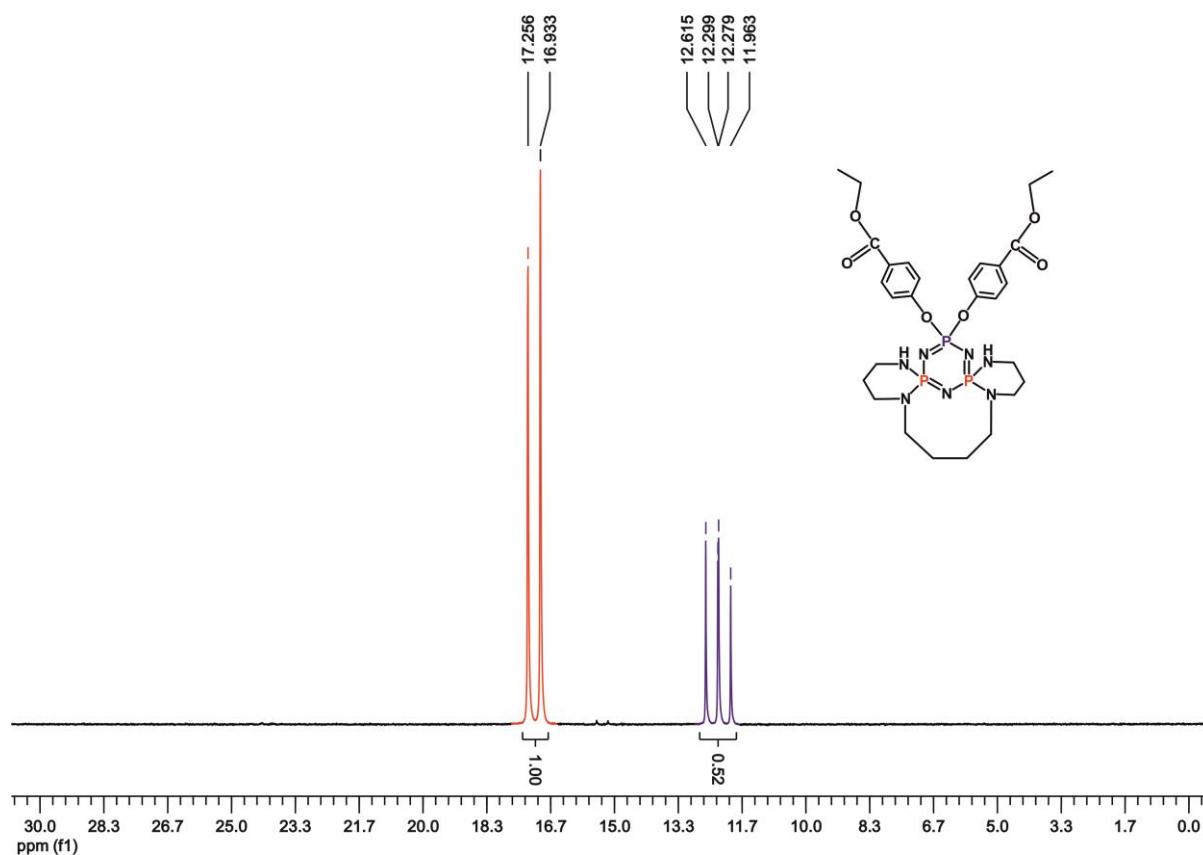


Figure S12: <sup>1</sup>H NMR spectrum of compound 3



**Figure S13:**  $^1\text{H}$  NMR spectrum of compound **3** after  $\text{D}_2\text{O}$  exchange



**Figure S14:** The proton decoupled  $^{31}\text{P}$  NMR spectrum of the compound **3**

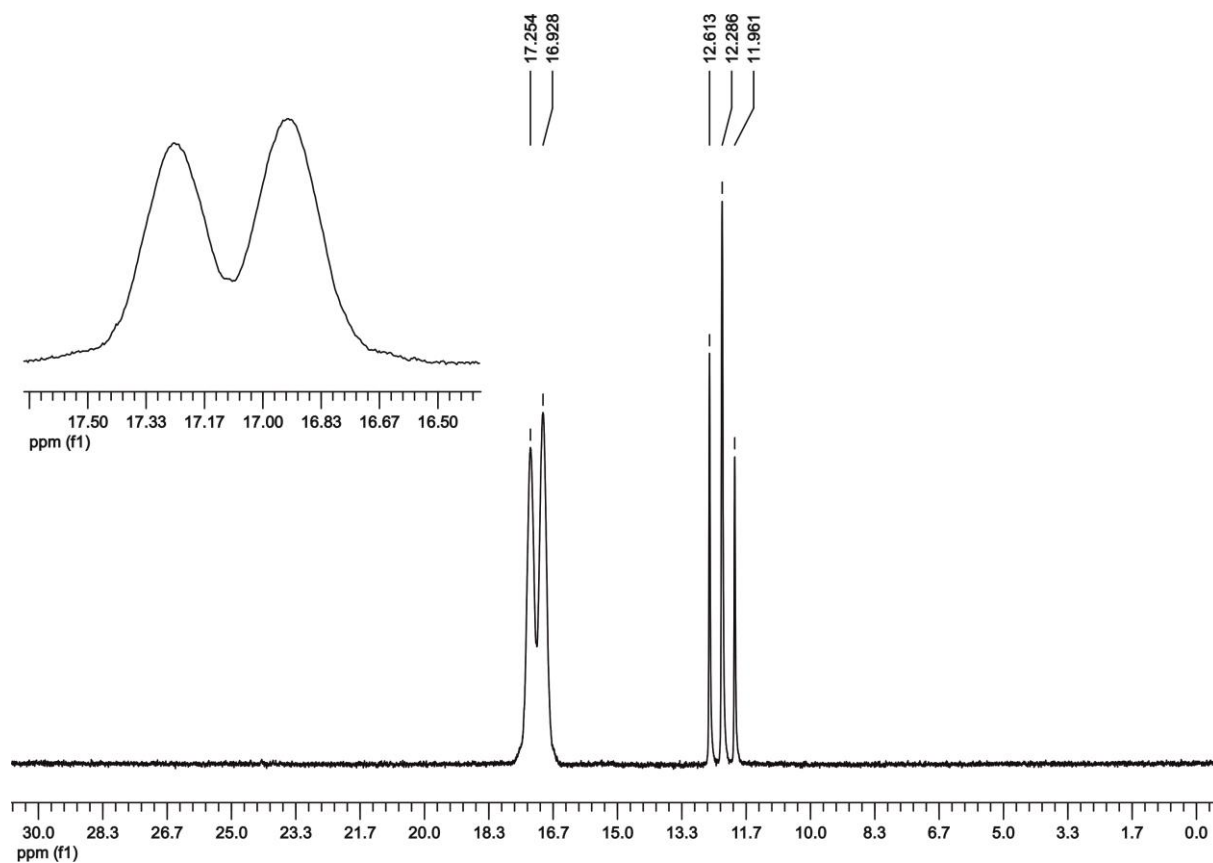


**Figure S15:** The proton coupled  $^{31}\text{P}$  NMR spectrum of the compound **3**

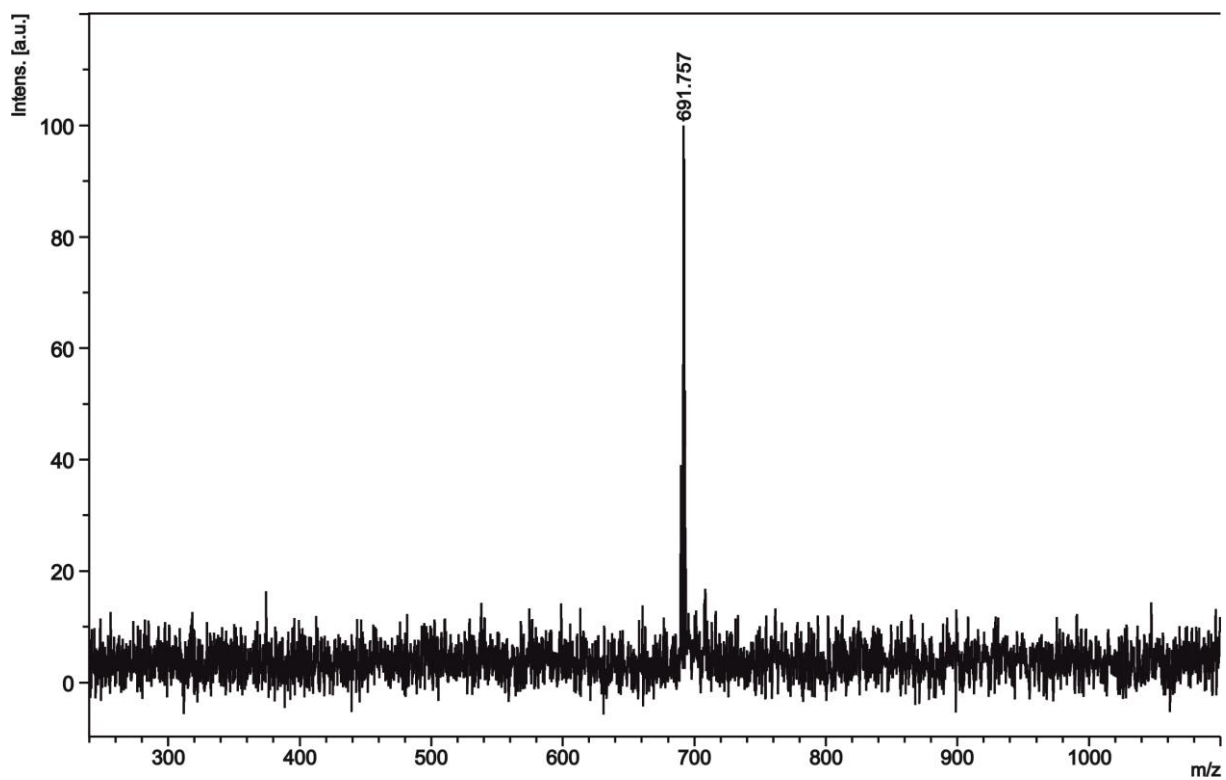


**Figure S16:** Mass spectrum of compound **4**

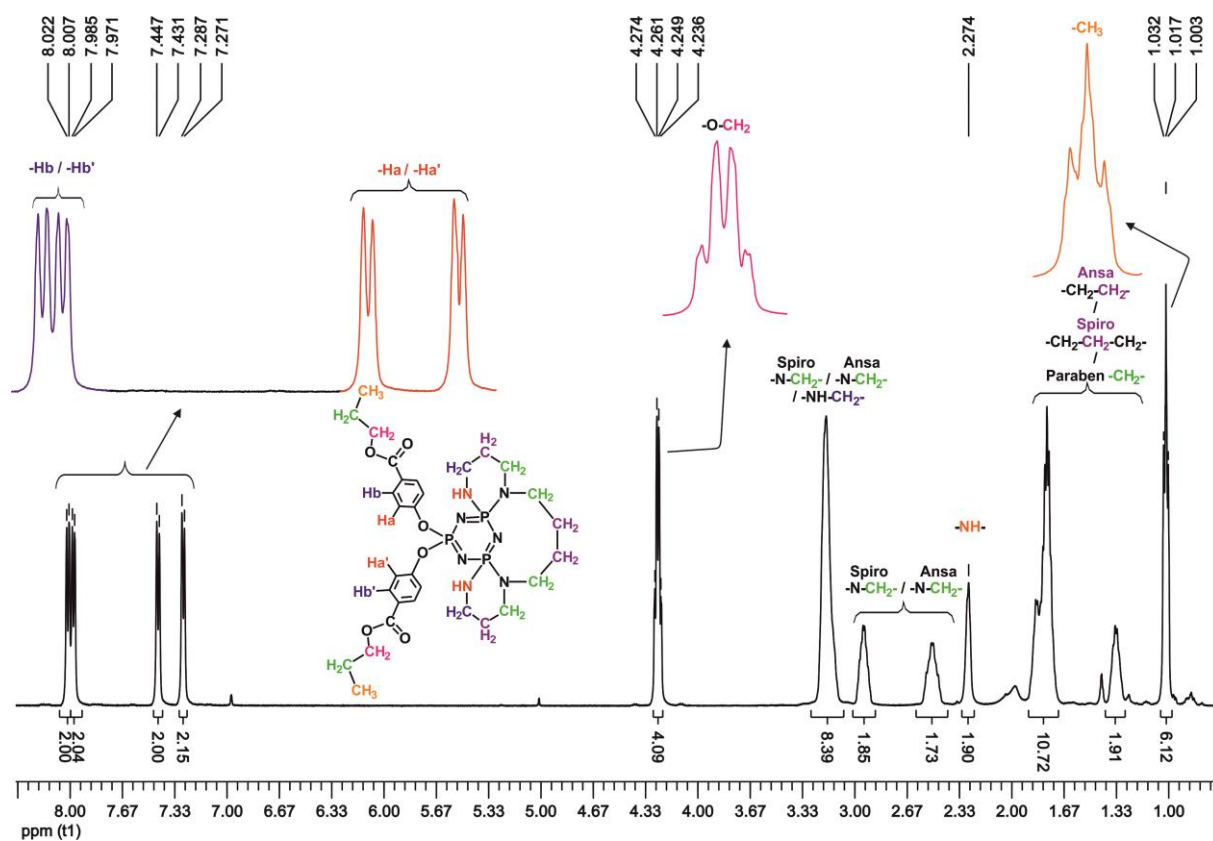


**Figure S17:** <sup>1</sup>H NMR spectrum of compound **4**

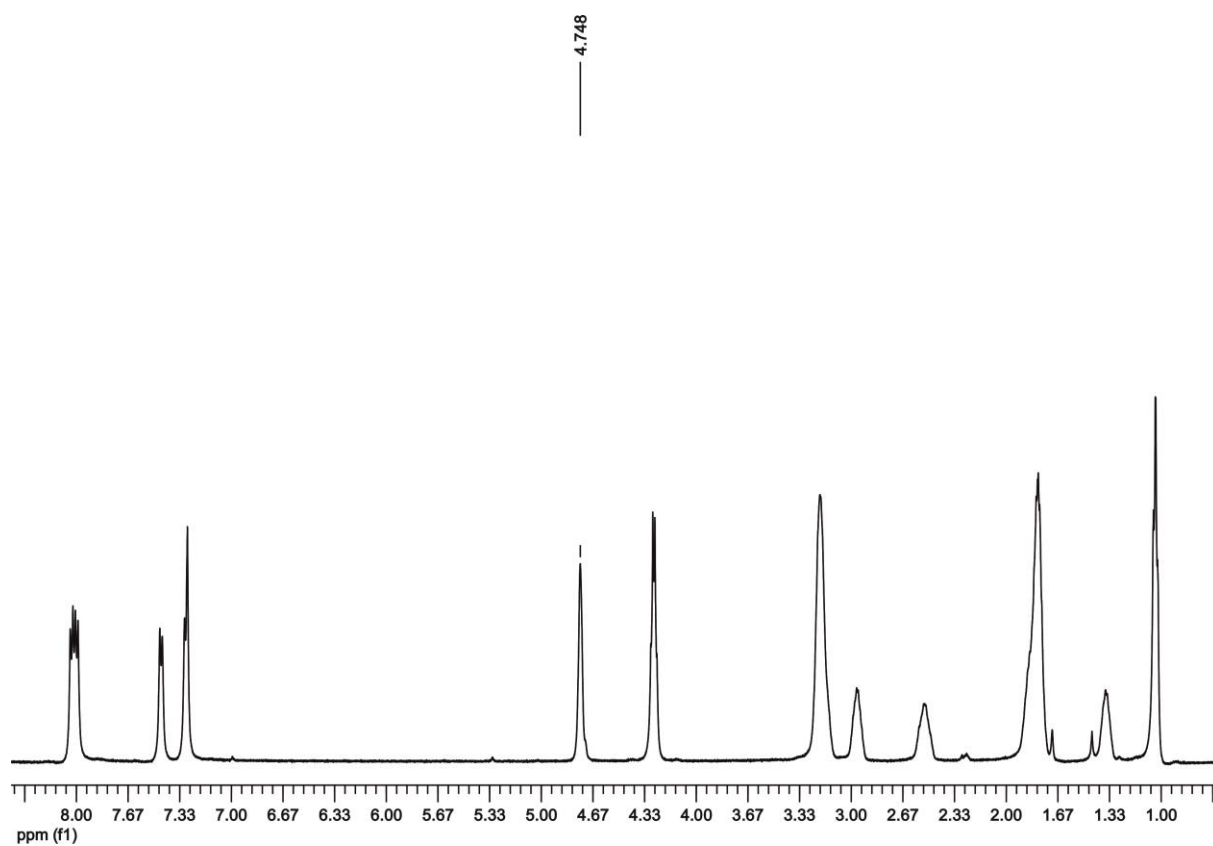


**Figure S18:** <sup>1</sup>H NMR spectrum of compound **4** after D<sub>2</sub>O exchange

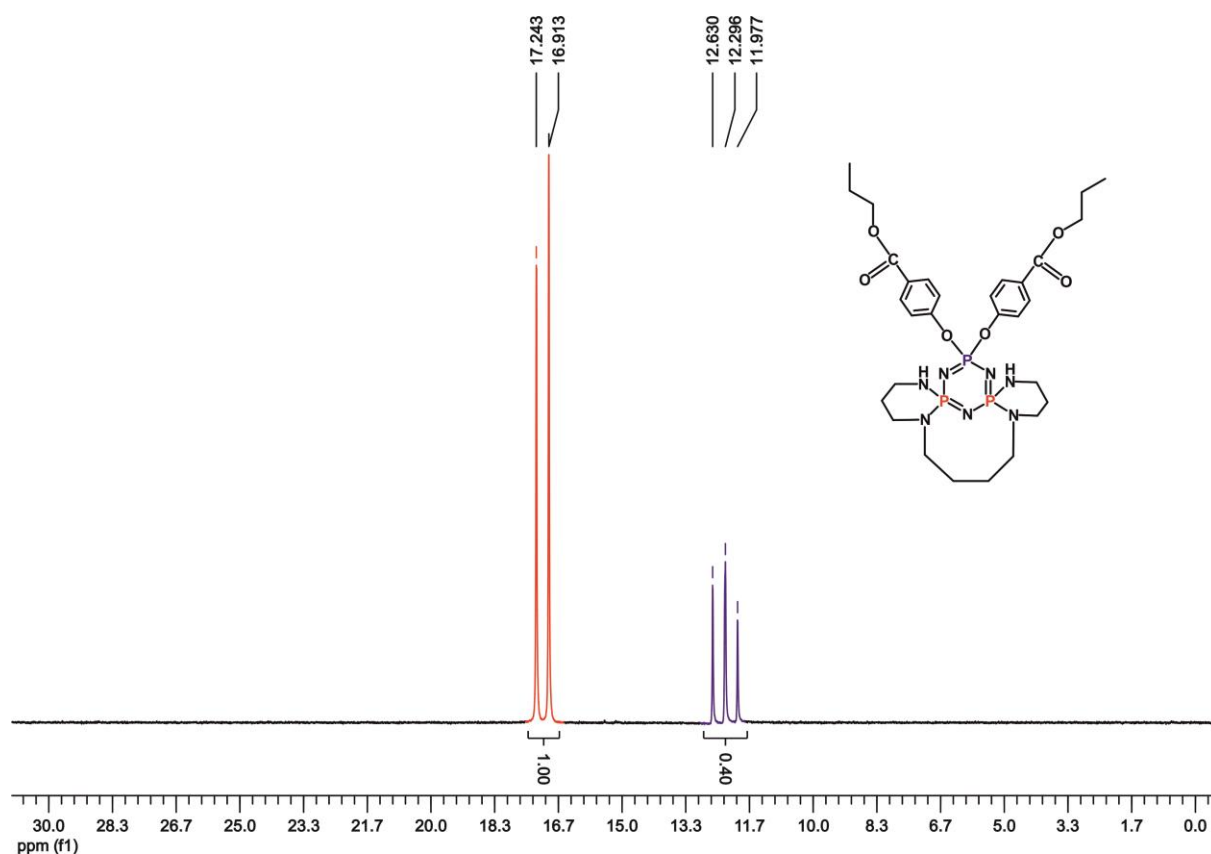


**Figure S19:** The proton decoupled  $^{31}\text{P}$  NMR spectrum of the compound **4**

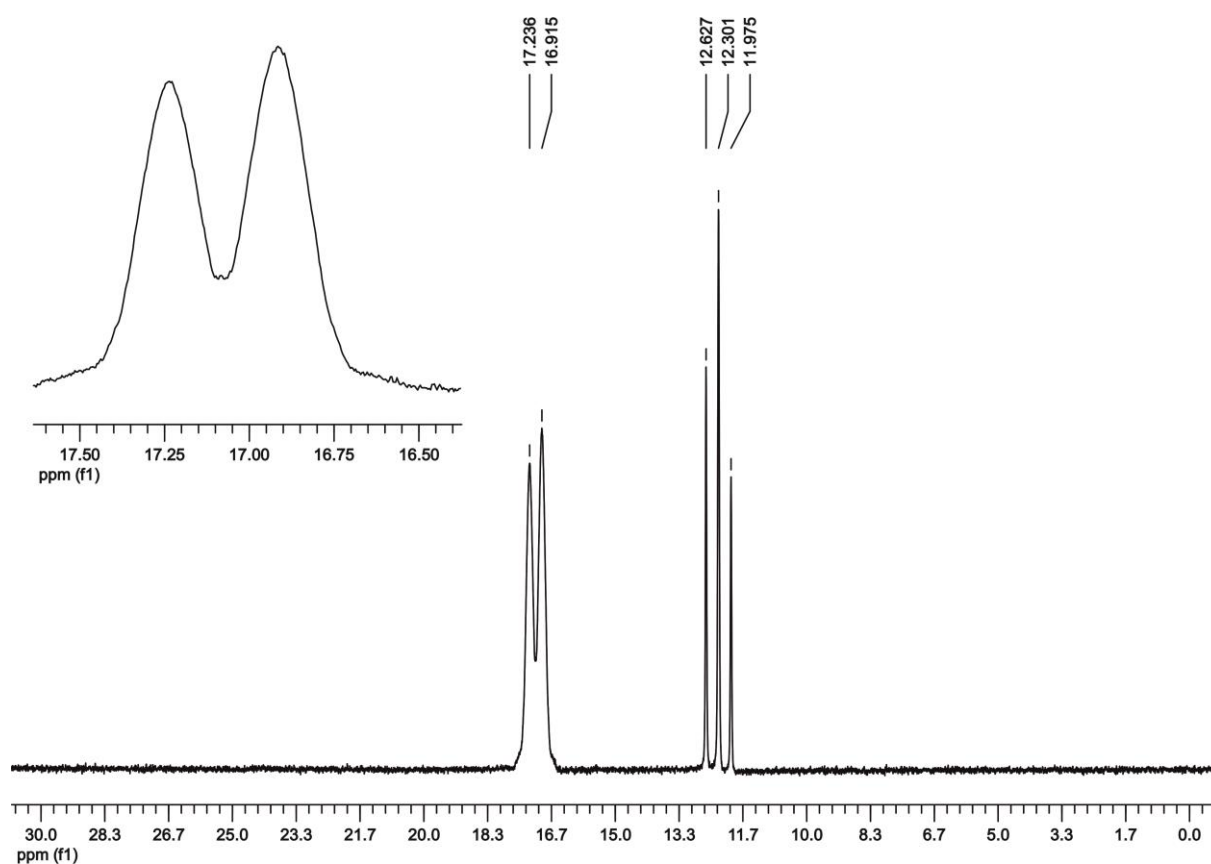


**Figure S20:** The proton coupled  $^{31}\text{P}$  NMR spectrum of the compound **4**



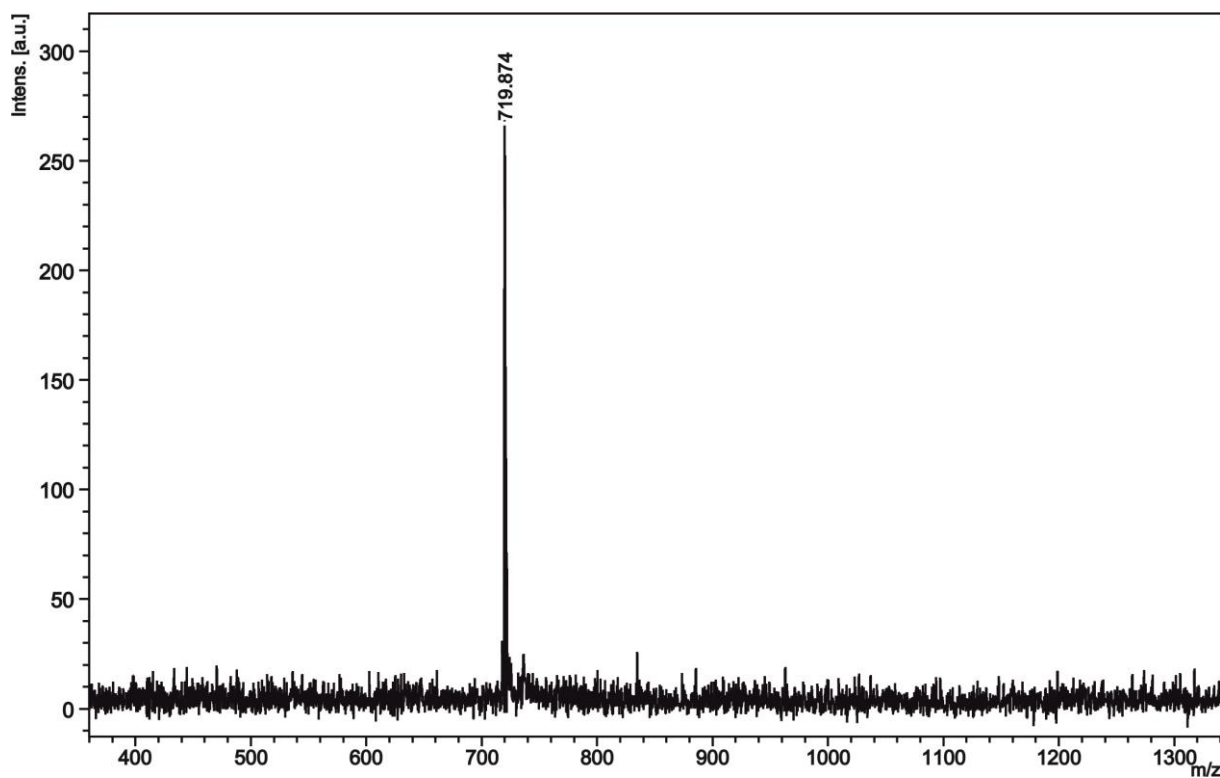


Figure S21: Mass spectrum of compound 5

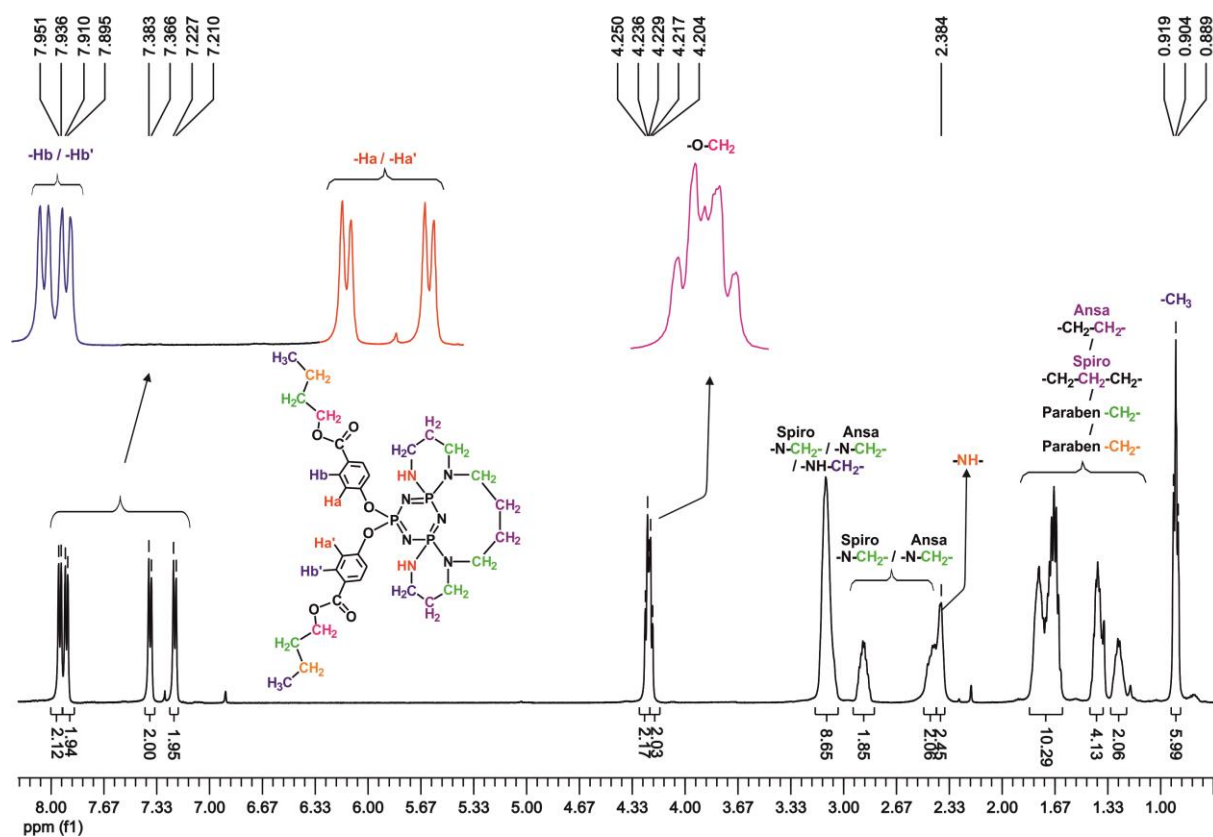
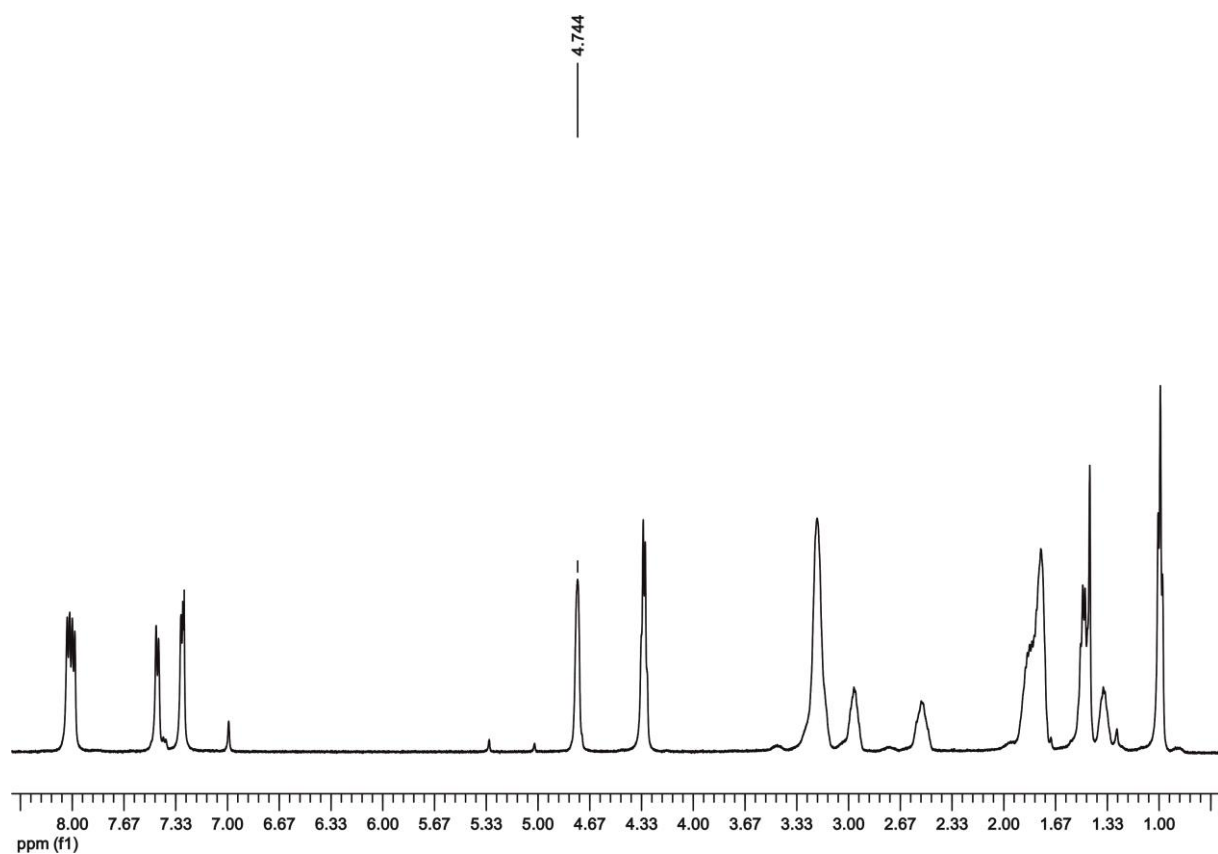
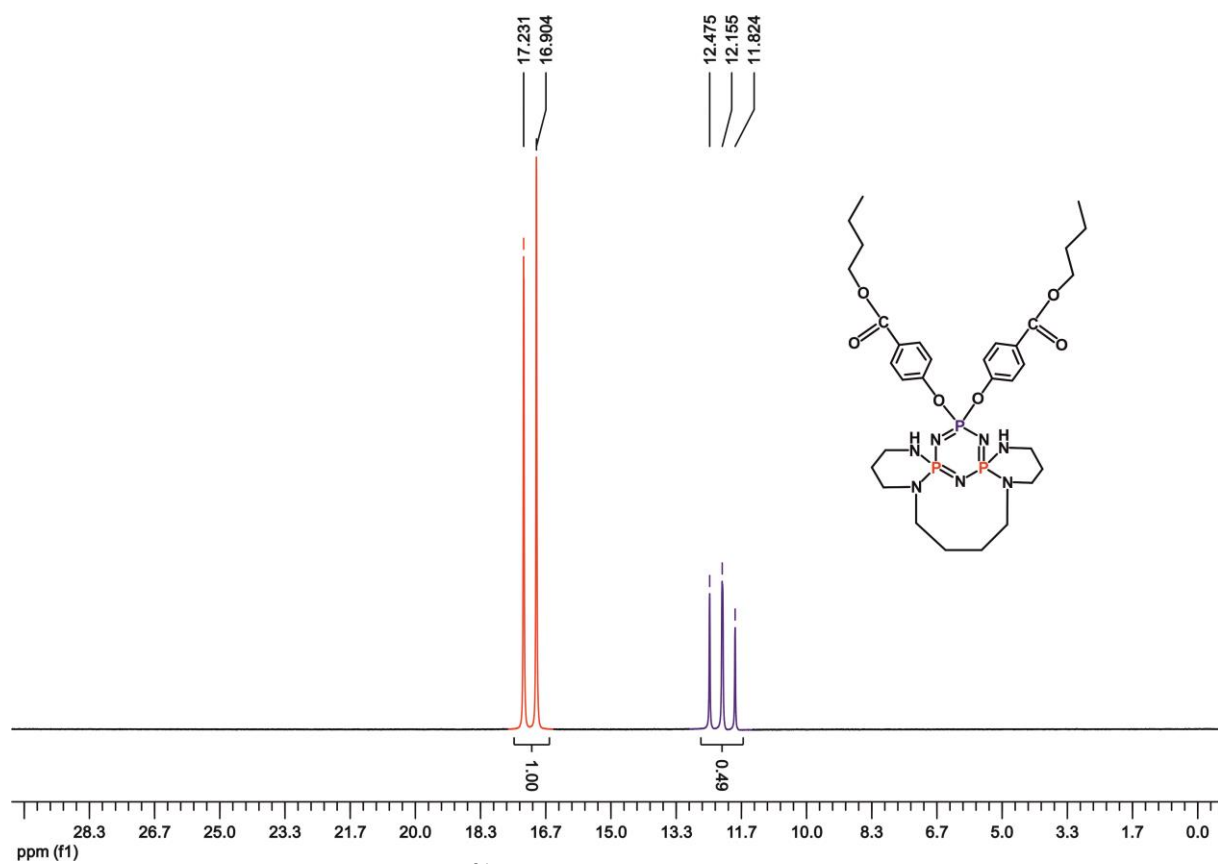


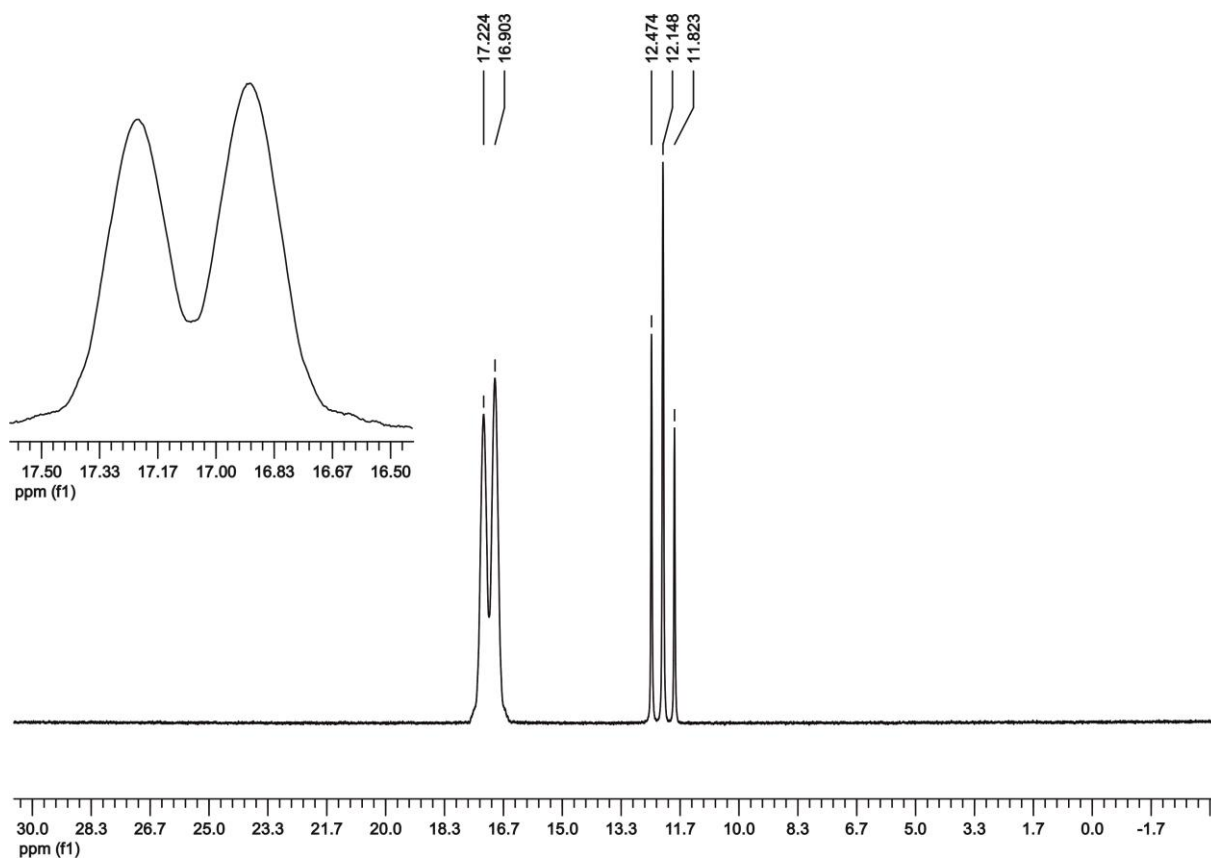
Figure S22: <sup>1</sup>H NMR spectrum of compound 5



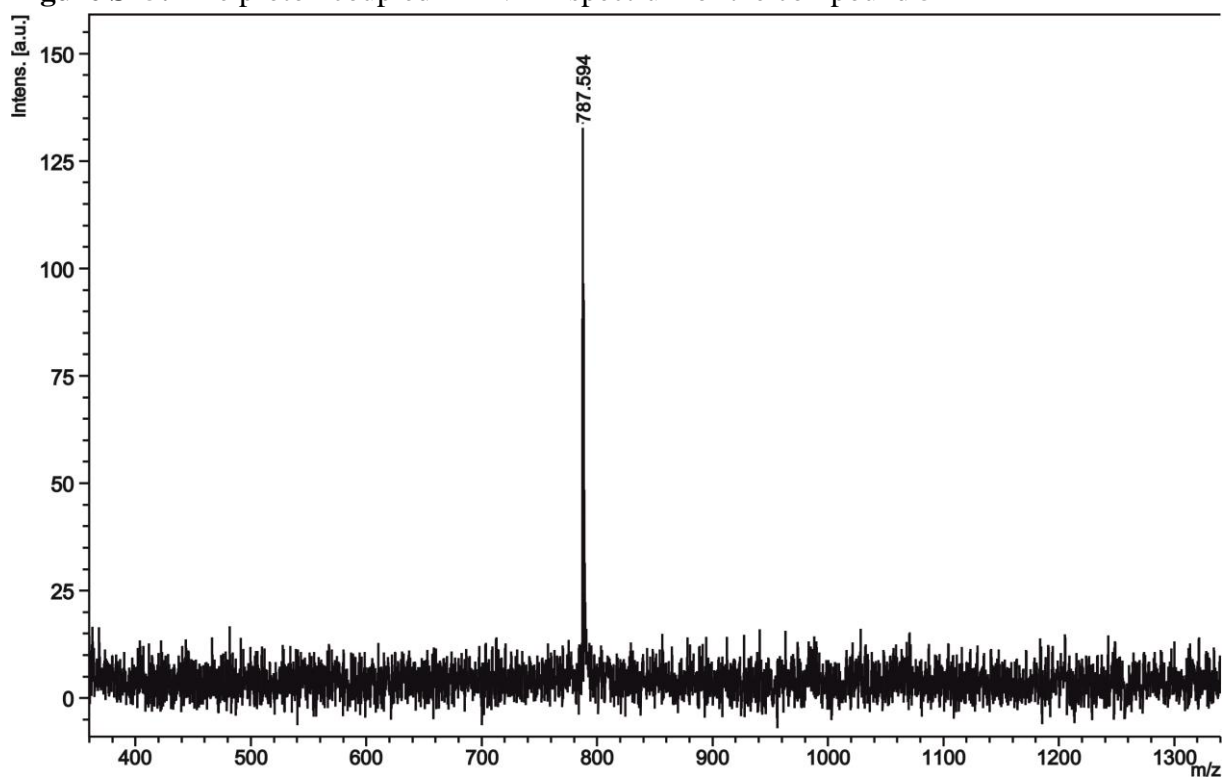
**Figure S23:**  $^1\text{H}$  NMR spectrum of compound **5** after  $\text{D}_2\text{O}$  exchange



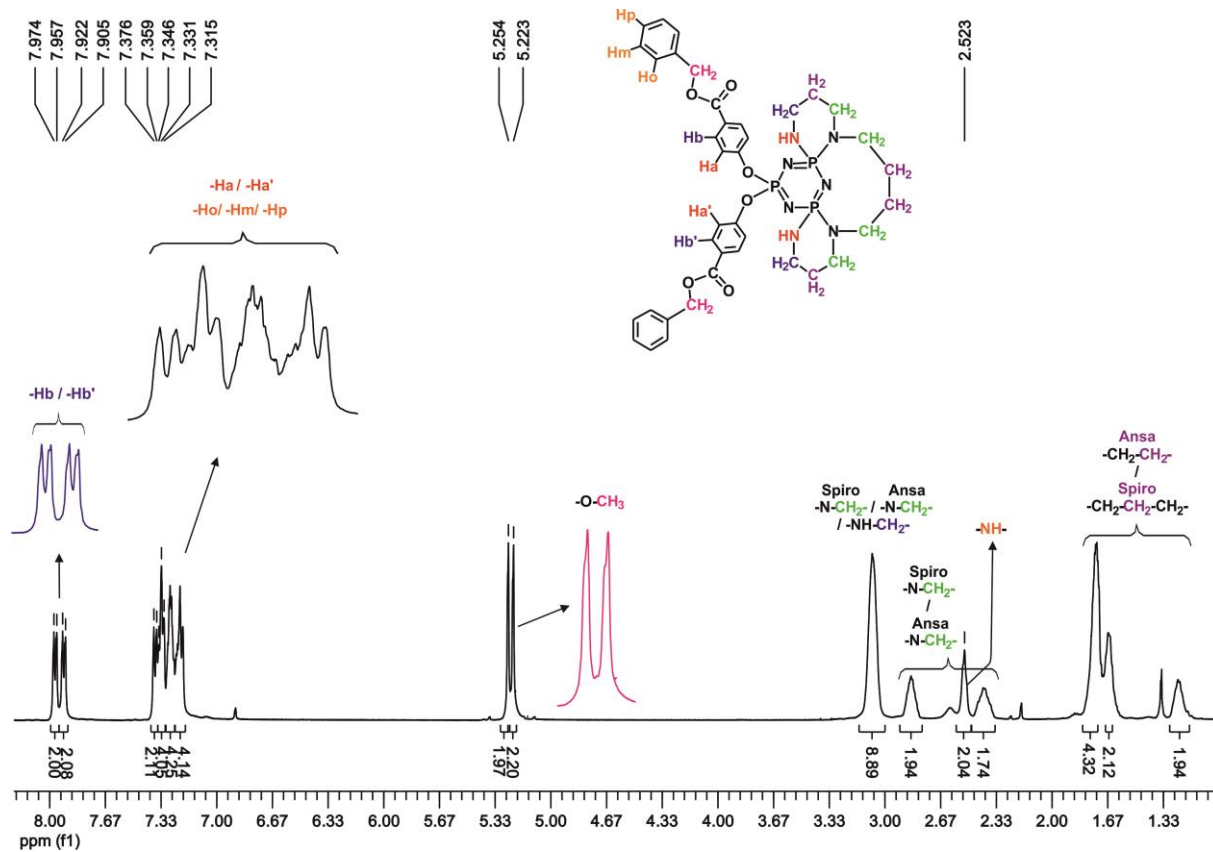
**Figure S24:** The proton decoupled  $^{31}\text{P}$  NMR spectrum of the compound **5**



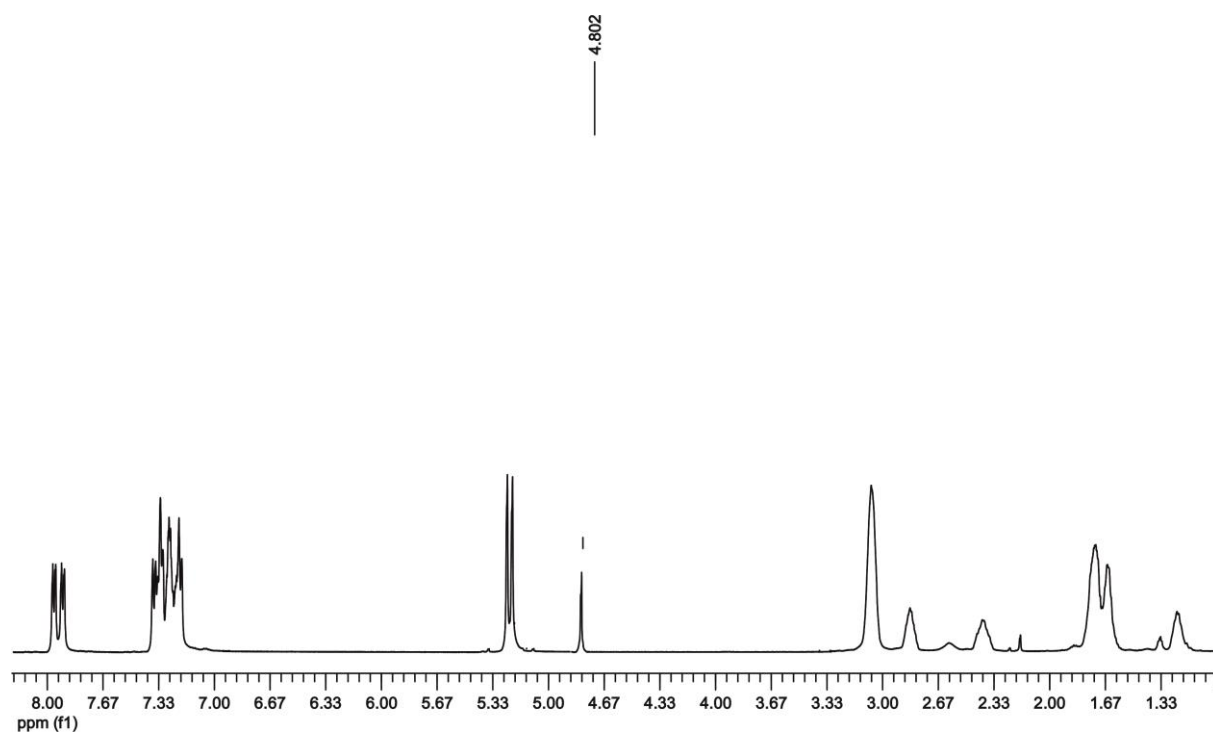
**Figure S25:** The proton coupled  $^{31}\text{P}$  NMR spectrum of the compound **5**



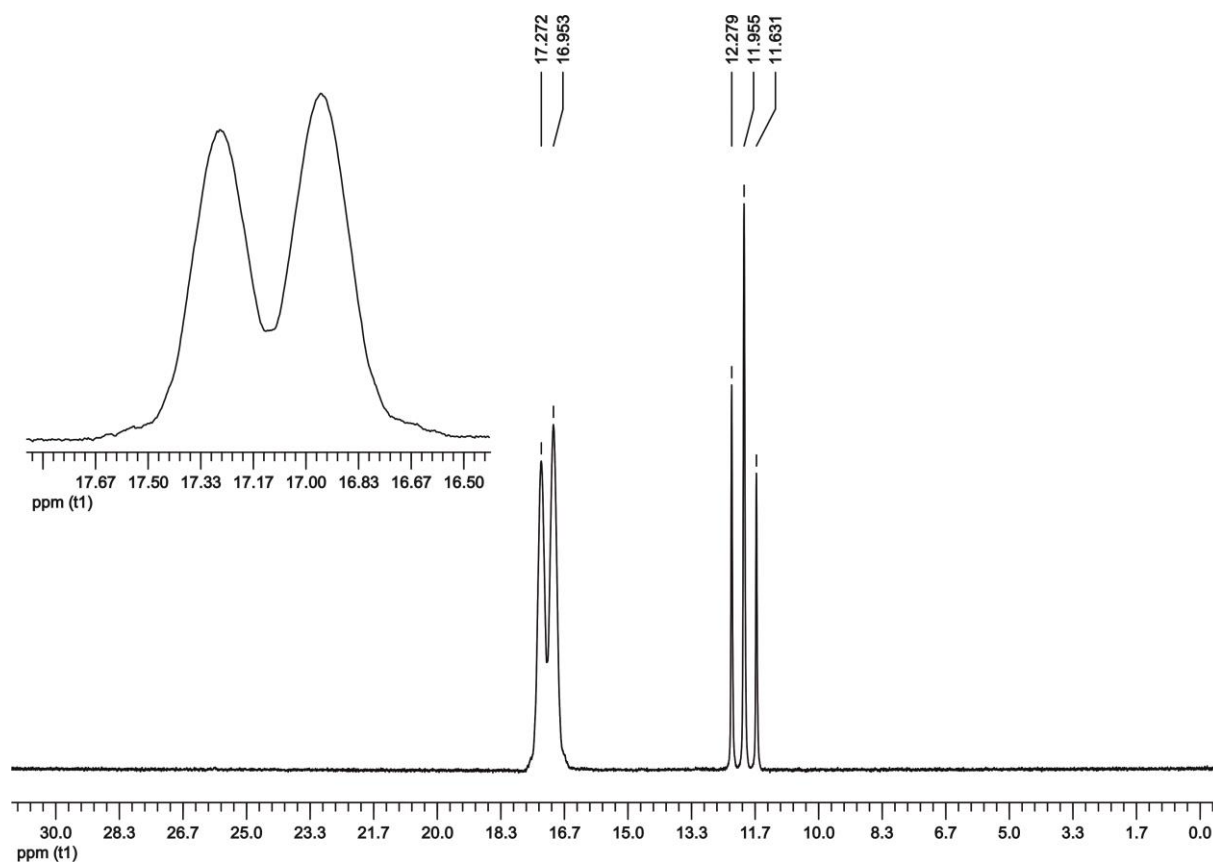
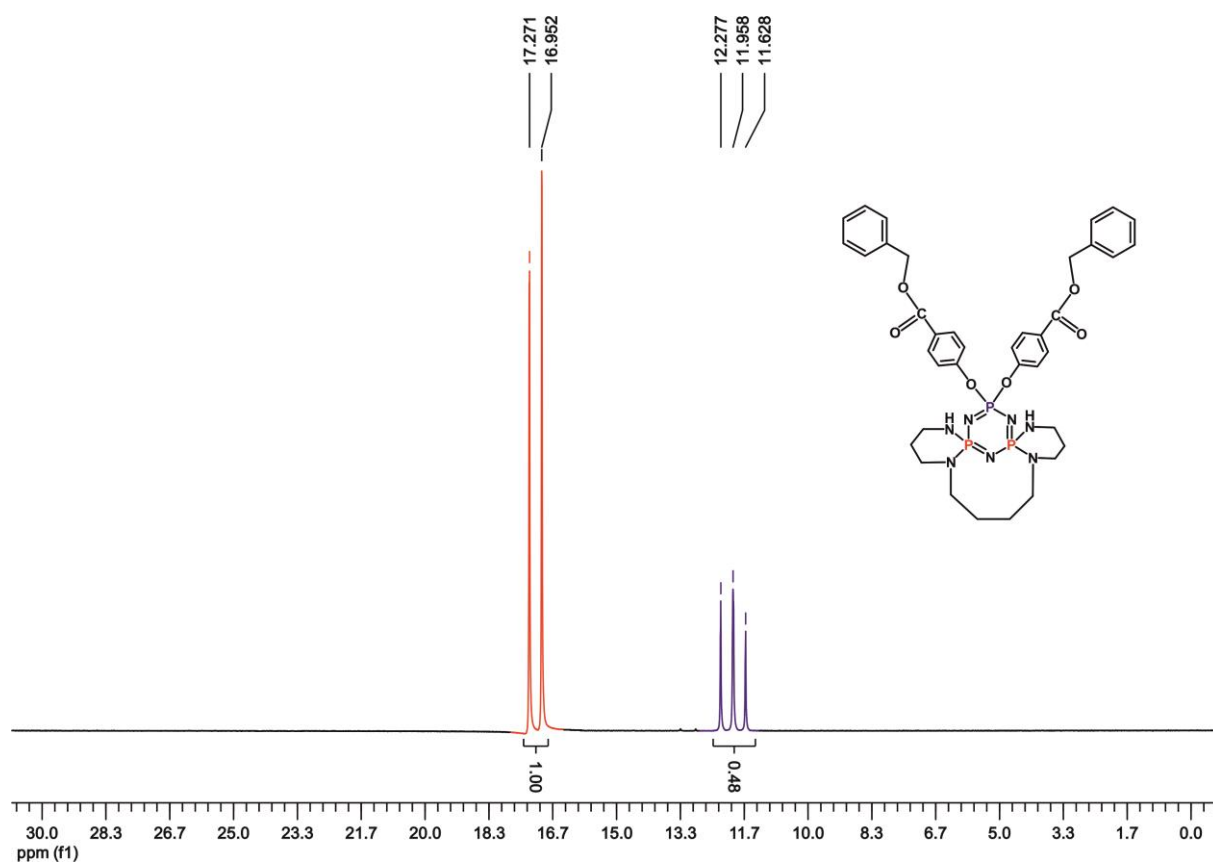
**Figure S26:** Mass spectrum of compound **6**



**Figure S27:** <sup>1</sup>H NMR spectrum of compound **6**



**Figure S28:** <sup>1</sup>H NMR spectrum of compound **6** after D<sub>2</sub>O exchange



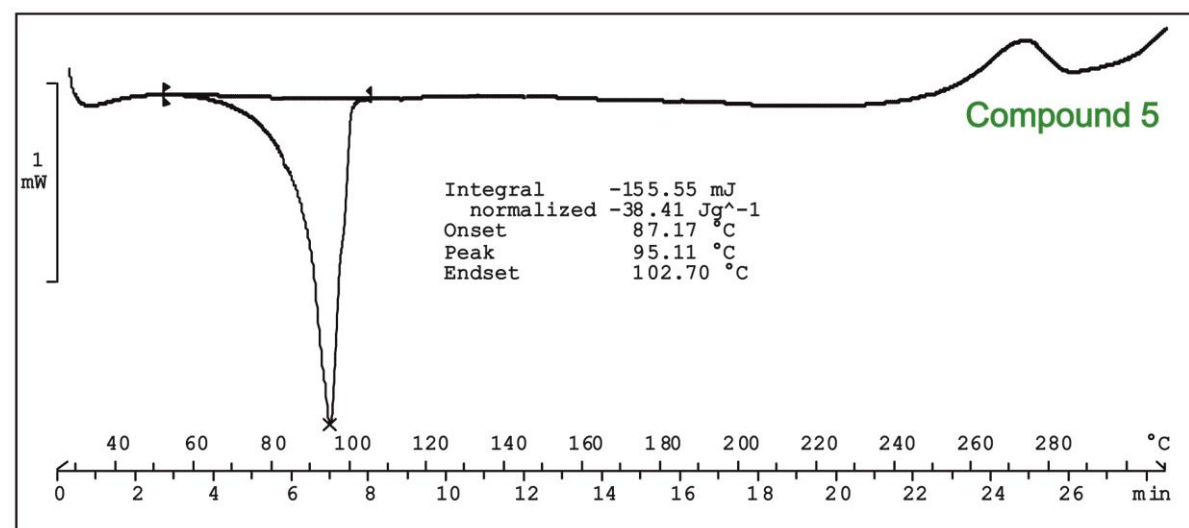
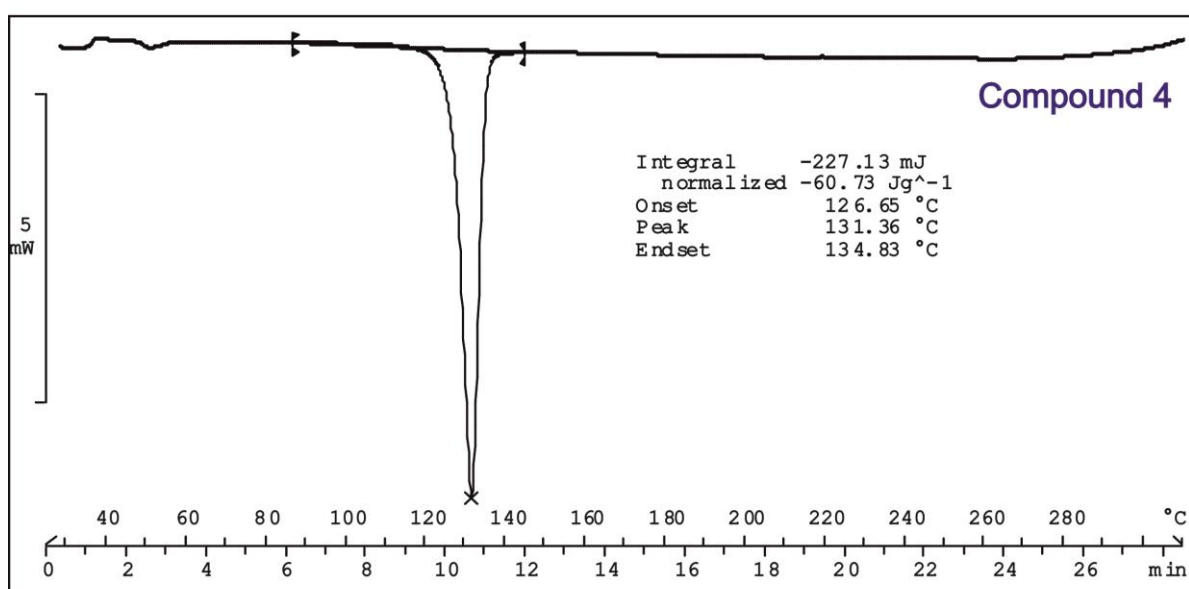
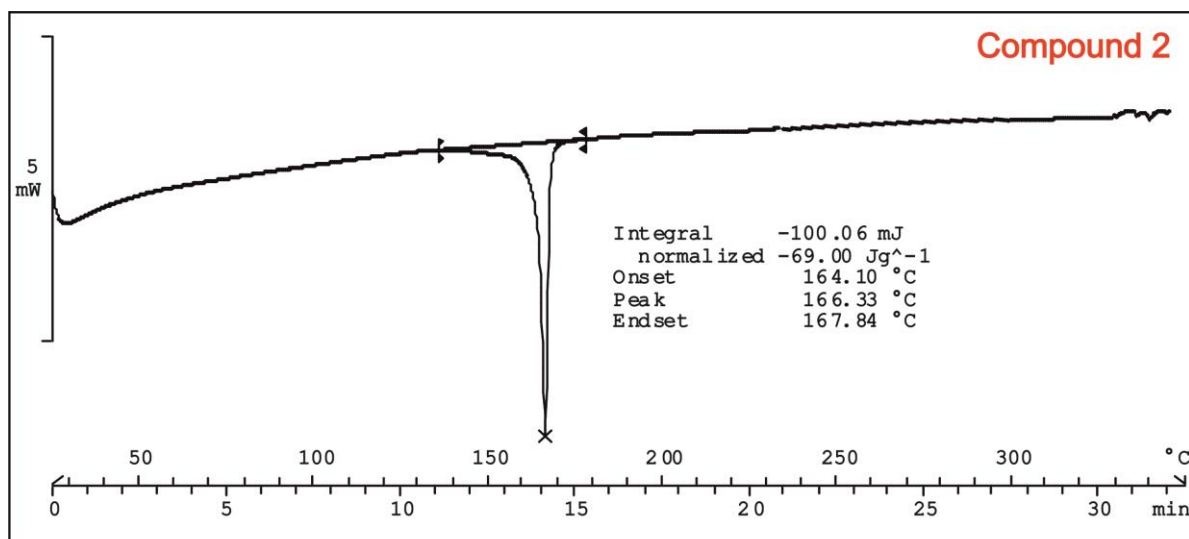


**Figure S31.** DSC curves of Compounds **2**, **4** and **5**.

**Table S1.** Selected bond lengths and bond angles of compounds **2**, **4** and **5**.

<b>Compound 2</b>			
<b>Bond Lengths (Å)</b>			
P1—N1	1.570 (6)	P2—N4	1.659 (7)
P1—N3	1.549 (6)	P2—N5	1.643 (7)
P2—N1	1.611 (6)	P3—N7	1.654 (7)
P2—N2	1.574 (6)	P3—N6	1.616 (7)
P3—N2	1.584 (6)	P1—O2	1.587 (5)
P3—N3	1.612 (7)	P1—O1	1.591 (5)
<b>Bond Angles (°)</b>			
P1—N1—P2	120.2 (3)	N3—P1—N1	119.3 (3)
P2—N2—P3	125.0 (4)	N2—P2—N1	114.7 (3)
P1—N3—P3	121.7 (4)	N2—P3—N3	113.5 (3)
<b>Compound 4</b>			
<b>Bond Lengths (Å)</b>			
P1—N3	1.568 (3)	P3—N7	1.637 (3)
P1—N1	1.571 (3)	P3—N6	1.662 (3)
P3—N3	1.609 (3)	P2—N4	1.647 (3)
P3—N2	1.590 (3)	P2—N5	1.655 (3)
P2—N2	1.581 (3)	P1—O1	1.593 (2)
P2—N1	1.604 (3)	P1—O2	1.594 (2)
<b>Bond Angles (°)</b>			
P1—N1—P2	121.2 (17)	N2—P3—N3	114.9 (14)
P1—N3—P3	120.6 (17)	N2—P2—N1	114.7 (14)
P3—N2—P2	124.1 (17)	N1—P1—N3	118.9 (15)
<b>Compound 5</b>			
<b>Bond Lengths (Å)</b>			
P1—N3	1.577 (4)	P3—N7	1.633 (6)
P1—N1	1.575 (5)	P3—N6	1.668 (4)
P3—N3	1.607 (5)	P2—N4	1.651 (5)
P3—N2	1.583 (5)	P2—N5	1.668 (5)
P2—N2	1.589 (5)	P1—O1	1.582 (4)
P2—N1	1.605 (5)	P1—O2	1.606 (4)
<b>Bond Angles (°)</b>			
P1—N1—P2	120.4 (3)	N2—P3—N3	114.7 (2)
P1—N3—P3	120.6 (3)	N2—P2—N1	115.0 (3)
P3—N2—P2	124.6 (3)	N1—P1—N3	119.1 (2)

**Table S2.** Selected conformational parameters of **2**, **3** and **5**

	<b>2</b>	<b>4</b>	<b>5</b>
<b>Deviation of N atoms (Å)</b>	0.078(6) (N1)	0.066(3) (N1)	0.077(5) (N1)
	<b>0.150(6) (N2)</b>	<b>0.147(3) (N2)</b>	<b>0.144(5) (N2)</b>
	0.069(7) (N3)	0.085(3) (N3)	0.084(5) (N3)
<b>Deviation of P atoms (Å)</b>	<b>0.148(3) (P1)</b>	<b>0.149(3) (P1)</b>	<b>0.155(2) (P1)</b>
	0.071(3) (P2)	0.083(12) (P2)	0.073(2) (P2)
	0.080(3) (P3)	0.063(12) (P3)	0.065(2) (P3)
<b>Q<sub>T</sub> (Å) for Phosphazene Ring</b>	0.258(5)	0.258(2)	0.260(4)

Q<sub>T</sub>: Total puckering amplitude**Table S3.** X-H... $\pi$  interactions for **2**, **4** and **5**.

Comp. No	X-H... Cg	Symmetry codes	H...Cg
<b>2</b>	C16-H16...Cg4	3/2-x, -1/2+y, 1/2-z	2.96
<b>4</b>	C18-H18...Cg4	-1+x, y, -1+z	2.94
<b>5</b>	C22-H22B...Cg4	-1+x, y, -1+z	2.97
	C28-H28B...Cg5	1+x, y, z	2.95

For **2**: Cg4: C1-C6, For **4**: Cg4, C1-C6, For **5**: Cg4, C1-C6; Cg5, C12-C17**Table S4.** Hydrogen bond parameters (Å and °) for **2**, **4** and **5**.

<b>Compound 2</b>					
<i>D-H...A</i>	Symmetry codes	<i>d(D-H)</i>	<i>d(H...A)</i>	<i>d(D-H...A)</i>	<i>D-H...A</i>
N5-H5...N1	1-x, 1-y, 1-z	1.00	2.43	3.405	164
C2-H2...N4	1-x, 1-y, 1-z	0.93	2.59	3.350	140
C18-H18A...O1	1-x, 1-y, 1-z	0.97	2.58	3.532	166
C23-H23B...N3		0.97	2.58	3.085	113
C25-H25...N2		0.97	2.61	3.267	125
<b>Compound 4</b>					
<i>D-H...A</i>	Symmetry codes	<i>d(D-H)</i>	<i>d(H...A)</i>	<i>d(D-H...A)</i>	<i>D-H...A</i>
N4-H4...N1		0.87	2.72	2.721	166
N7-H7...N3	1-x, 2-y, 1-z	0.77	2.65	3.418	169
C10-H10A...O3		0.96	2.43	2.850	106
C12-H12...N6	1-x, 2-y, 1-z	0.93	2.57	3.361	143
C22-H22A...O2	1-x, 2-y, 1-z	0.97	2.52	3.482	171
C25-H25A...N2		0.97	2.58	3.240	125
C27-H27B...N1		0.97	2.62	3.110	112
<b>Compound 5</b>					



<i>D-H...A</i>	Symmetry codes	<i>d(D-H)</i>	<i>d(H...A)</i>	<i>d(D-H...A)</i>	<i>D-H...A</i>
N7-H7...N3	1-x, 2-y, 1-z	0.85	2.50	3.328	168
N4-H4...N1		0.91	2.74	3.615	160
C20-H20A...O4	1-x, 2-y, 1-z	0.97	2.49	3.267	137
C24-H24B...O2	1-x, 2-y, 1-z	0.97	2.47	3.423	169
C27-H27A...N2		0.97	2.61	3.254	124
C29-H29B...N1		0.97	2.62	3.116	112

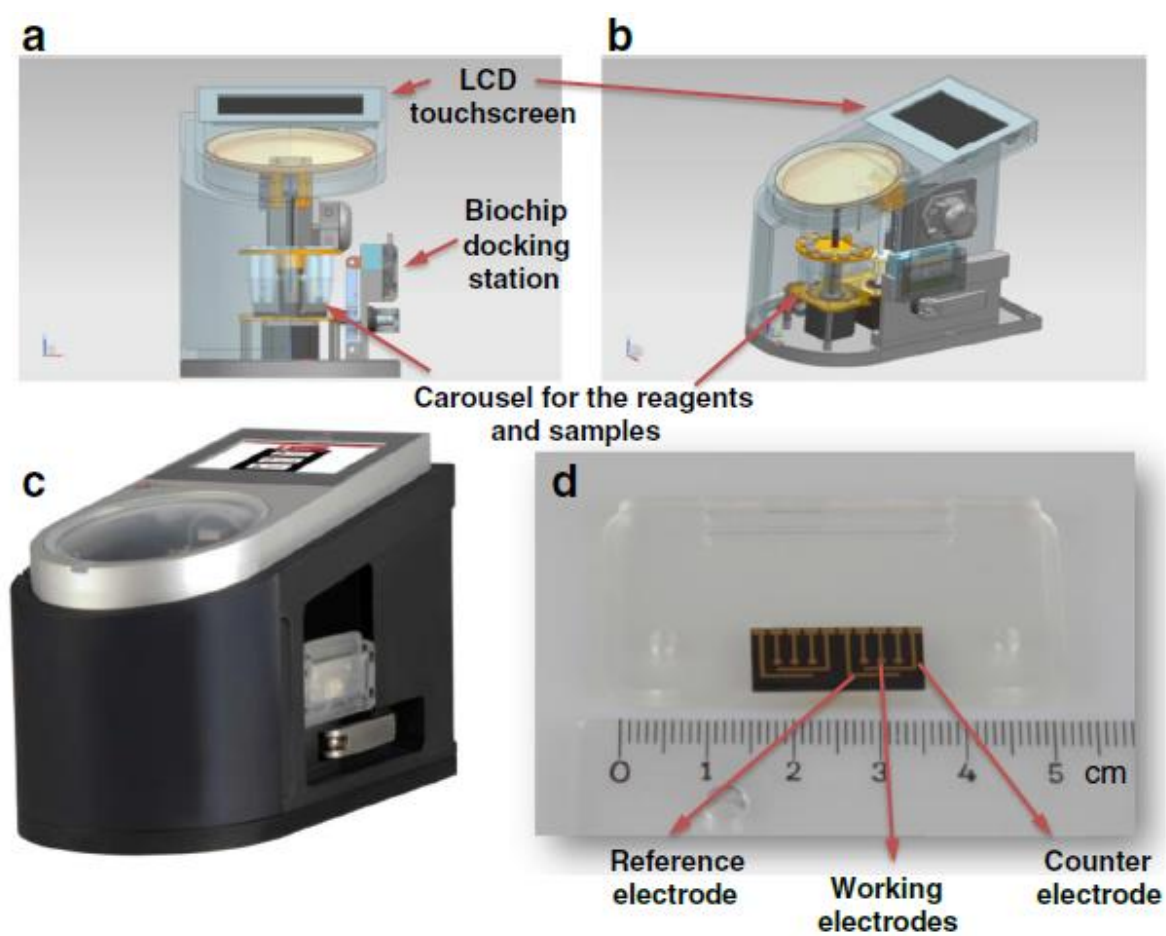


**Figure S32.** Fully integrated and b automated Biosensor device (a-b-c) and its biochip (d)

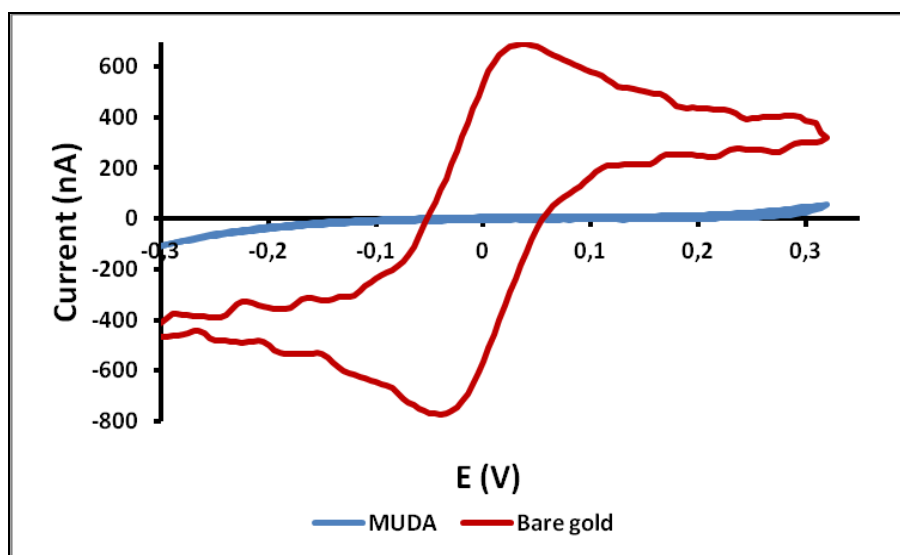


**Figure S33.** The cyclic voltammetry using bare and MUDA coated gold electrode arrays (1 mM  $K_4[Fe(CN)_6]/KCl$  at 100 mV/s scan rate).

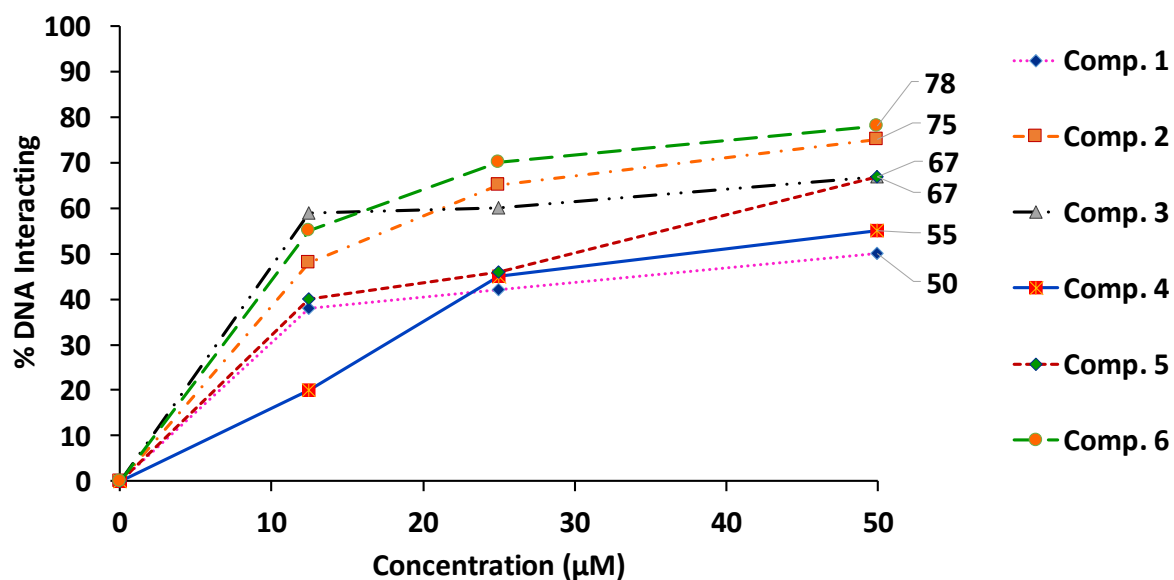


**Figure S34.** The amperometric responses were shown as percent relative hybridization responses in the figure, percentages of interacting DNA are shown (Compounds at 0, 12.5, 25 and 50  $\mu M$  concentrations were incubated with DNA probes before injection onto the biochip).

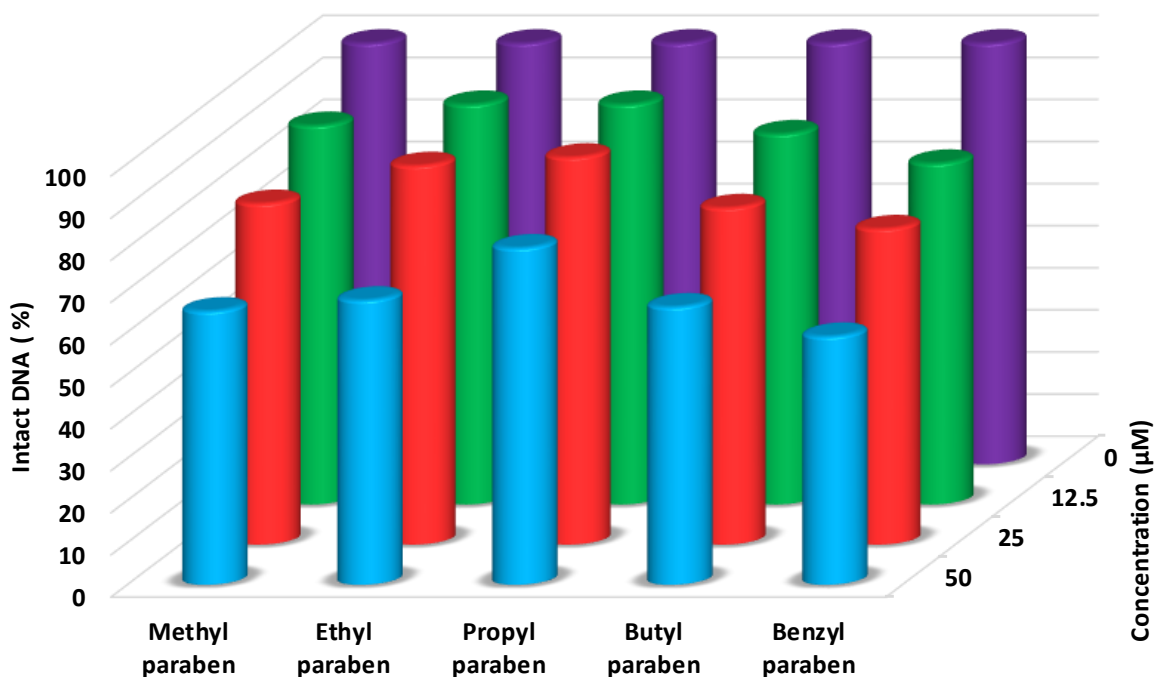


**Figure S35.** The amperometric responses were shown as percent relative hybridization responses in the figure, indicated by remaining from interaction DNA of Parabens (0, 12.5, 25 and 50  $\mu\text{M}$ ) were incubated with DNA probes prior to the injection on to the biochip.

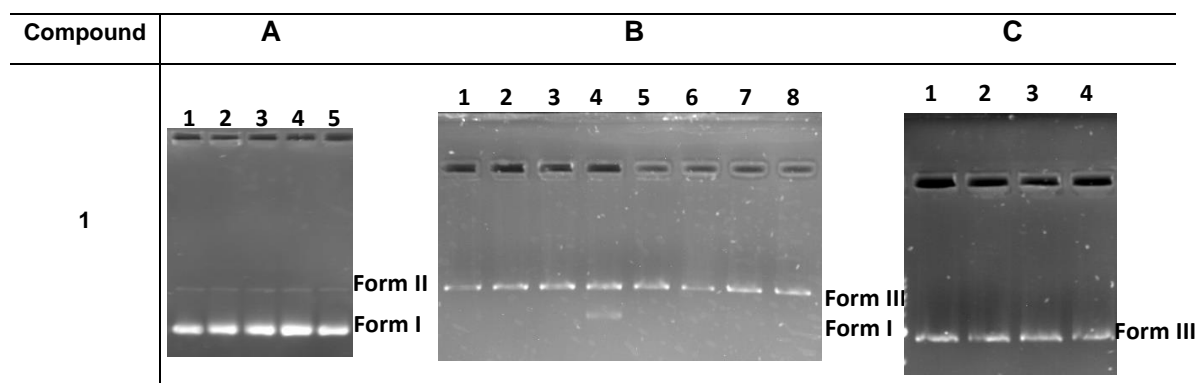


**Figure S36.** Agarose gel images of pUC18 plasmid DNA when incubated with different concentrations of compound **1** and EcoRI, HindIII and BamHI digested mixtures of pUC18 plasmid DNA after treatment with various concentrations of compounds **1**. Gels at the A line: lane 1, TE; lane 2, DMSO (0.1%); lanes 3–5, 12.5–25–50  $\mu\text{M}$ . Gels at the B line: lane 1, BamHI-treated pUC18 plasmid DNA in 0.1% DMSO; lanes 2–4, BamHI-treated pUC18 plasmid DNA interacting with increasing concentrations of the compound (12.5–50  $\mu\text{M}$ ); lane 5, EcoRI-treated pUC18 plasmid DNA in 0.1% DMSO; lanes 6–8, EcoRI-treated pUC18 plasmid DNA interacting with increasing concentrations of the compound (from 12.5 to 50  $\mu\text{M}$ ). Gels at the C line: lane 1, HindIII-treated pUC18 plasmid DNA in 0.1% DMSO; lanes 2–4, HindIII-treated pUC18 plasmid DNA interacting with increasing concentrations of the compound (12.5–50  $\mu\text{M}$ ).

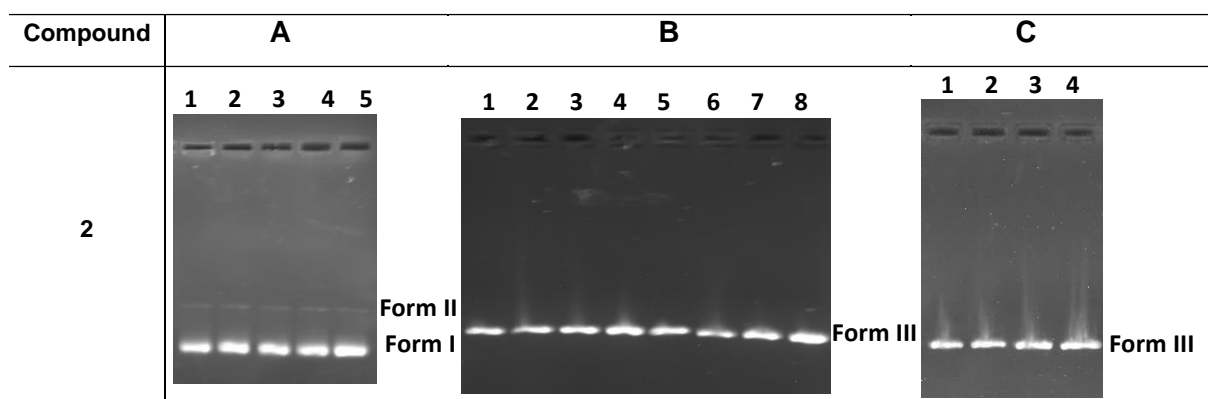


**Figure S37.** Agarose gel images of pUC18 plasmid DNA when incubated with different concentrations of compound **2** and EcoRI, HindIII and BamHI digested mixtures of pUC18 plasmid DNA after treatment with various concentrations of compounds **2**. Gels at the A line: lane 1, TE; lane 2, DMSO (0.1%); lanes 3–5, 12.5–25–50  $\mu\text{M}$ . Gels at the B line: lane 1, BamHI-treated pUC18 plasmid DNA in 0.1% DMSO; lanes 2–4, BamHI-treated pUC18 plasmid DNA interacting with increasing concentrations of the compound (12.5–50  $\mu\text{M}$ ); lane 5, EcoRI-treated pUC18 plasmid DNA in 0.1% DMSO; lanes 6–8, EcoRI-treated pUC18 plasmid DNA interacting with increasing concentrations of the compound (from 12.5 to 50  $\mu\text{M}$ ). Gels at the C line: lane 1, HindIII-treated pUC18 plasmid DNA in 0.1% DMSO; lanes 2–4, HindIII-treated pUC18 plasmid DNA interacting with increasing concentrations of the compound (12.5–50  $\mu\text{M}$ ).

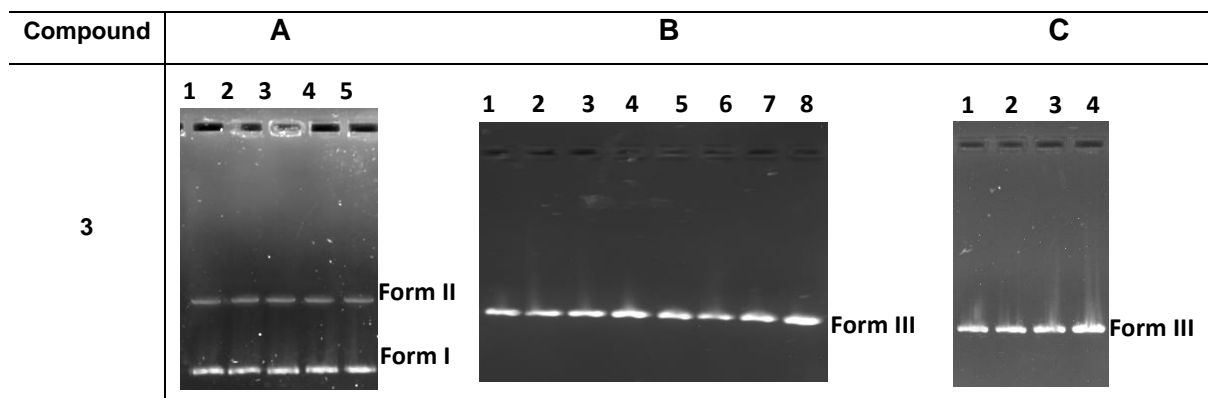


**Figure S38.** Agarose gel images of pUC18 plasmid DNA when incubated with different concentrations of compound **3** and EcoRI, HindIII and BamHI digested mixtures of pUC18 plasmid DNA after treatment with various concentrations of compounds **3**. Gels at the A line: lane 1, TE; lane 2, DMSO (0.1%); lanes 3–5, 12.5–25–50  $\mu\text{M}$ . Gels at the B line: lane 1, BamHI-treated pUC18 plasmid DNA in 0.1% DMSO; lanes 2–4, BamHI-treated pUC18 plasmid DNA interacting with increasing concentrations of the compound (12.5–50  $\mu\text{M}$ ); lane 5, EcoRI-treated pUC18 plasmid DNA in 0.1% DMSO; lanes 6–8, EcoRI-treated pUC18 plasmid DNA interacting with increasing concentrations of the compound (from 12.5 to 50  $\mu\text{M}$ ). Gels at the C line: lane 1, HindIII-treated pUC18 plasmid DNA in 0.1% DMSO; lanes 2–4, HindIII-treated pUC18 plasmid DNA interacting with increasing concentrations of the compound (12.5–50  $\mu\text{M}$ ).

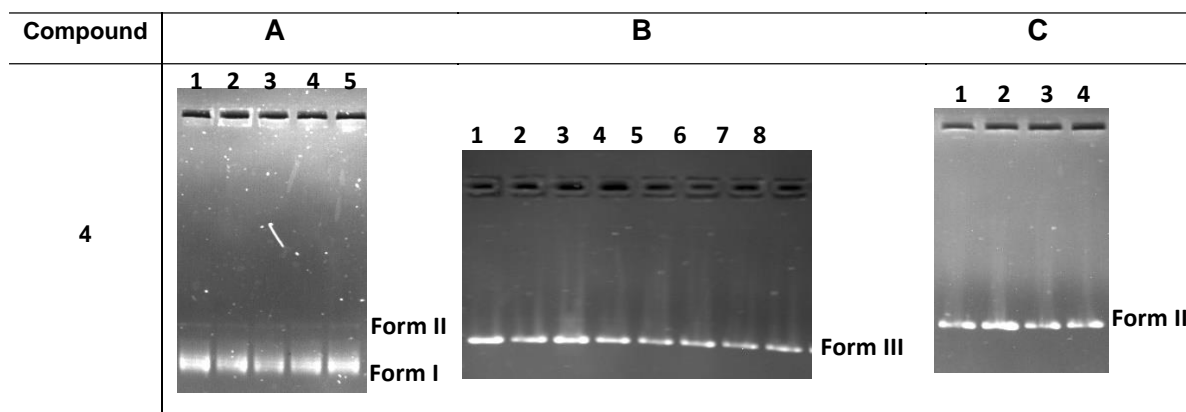


**Figure S39.** Agarose gel images of pUC18 plasmid DNA when incubated with different concentrations of compound **4** and EcoRI, HindIII and BamHI digested mixtures of pUC18 plasmid DNA after treatment with various concentrations of compounds **4**. Gels at the A line: lane 1, TE; lane 2, DMSO (0.1%); lanes 3–5, 12.5–25–50  $\mu$ M. Gels at the B line: lane 1, BamHI-treated pUC18 plasmid DNA in 0.1% DMSO; lanes 2–4, BamHI-treated pUC18 plasmid DNA interacting with increasing concentrations of the compound (12.5–50  $\mu$ M); lane 5, EcoRI-treated pUC18 plasmid DNA in 0.1% DMSO; lanes 6–8, EcoRI-treated pUC18 plasmid DNA interacting with increasing concentrations of the compound (from 12.5 to 50  $\mu$ M). Gels at the C line: lane 1, HindIII-treated pUC18 plasmid DNA in 0.1% DMSO; lanes 2–4, HindIII-treated pUC18 plasmid DNA interacting with increasing concentrations of the compound (12.5–50  $\mu$ M).

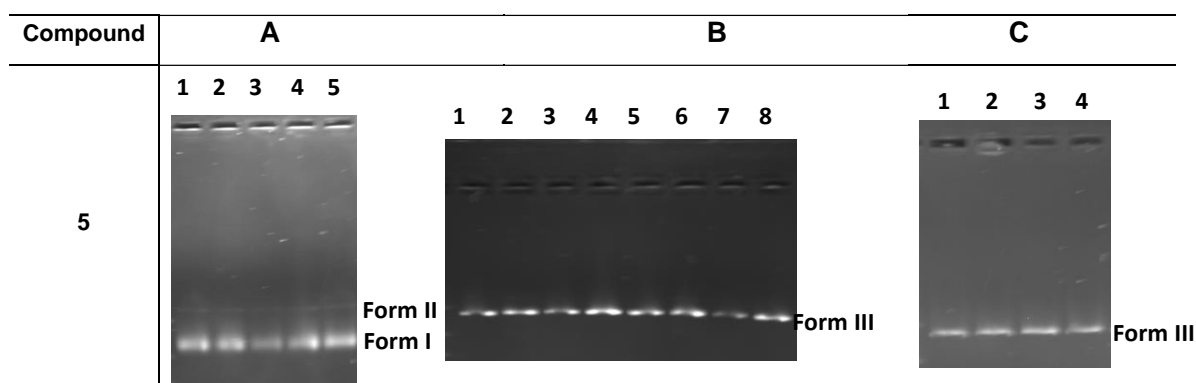


**Figure S40.** Agarose gel images of pUC18 plasmid DNA when incubated with different concentrations of compound **5** and EcoRI, HindIII and BamHI digested mixtures of pUC18 plasmid DNA after treatment with various concentrations of compounds **5**. Gels at the A line: lane 1, TE; lane 2, DMSO (0.1%); lanes 3–5, 12.5–25–50  $\mu$ M. Gels at the B line: lane 1, BamHI-treated pUC18 plasmid DNA in 0.1% DMSO; lanes 2–4, BamHI-treated pUC18 plasmid DNA interacting with increasing concentrations of the compound (12.5–50  $\mu$ M); lane 5, EcoRI-treated pUC18 plasmid DNA in 0.1% DMSO; lanes 6–8, EcoRI-treated pUC18 plasmid DNA interacting with increasing concentrations of the compound (from 12.5 to 50  $\mu$ M). Gels at the C line: lane 1, HindIII-treated pUC18 plasmid DNA in 0.1% DMSO; lanes 2–4, HindIII-treated pUC18 plasmid DNA interacting with increasing concentrations of the compound (12.5–50  $\mu$ M).

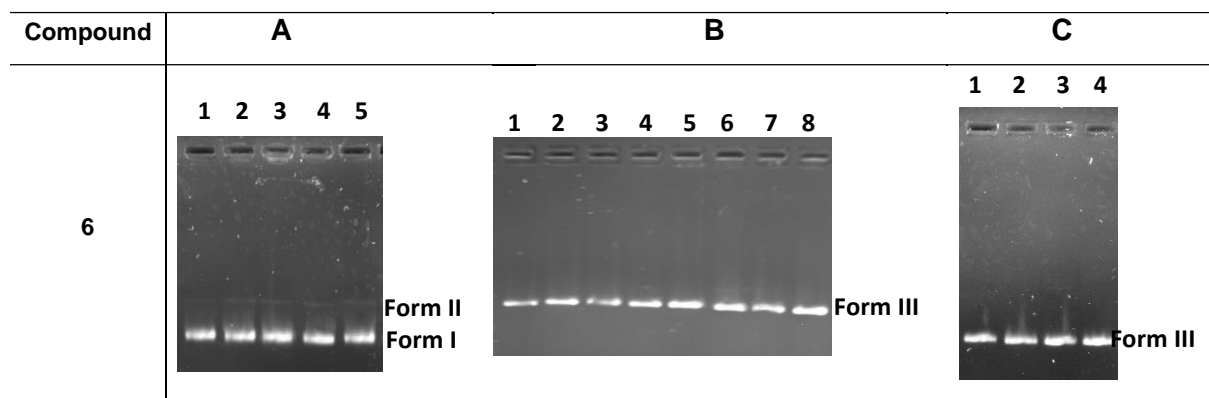


**Figure S41.** Agarose gel images of pUC18 plasmid DNA when incubated with different concentrations of compound **6** and EcoRI, HindIII and BamHI digested mixtures of pUC18 plasmid DNA after treatment with various concentrations of compounds **6**. Gels at the A line: lane 1, TE; lane 2, DMSO (0.1%); lanes 3–5, 12.5–25–50  $\mu\text{M}$ . Gels at the B line: lane 1, BamHI-treated pUC18 plasmid DNA in 0.1% DMSO; lanes 2–4, BamHI-treated pUC18 plasmid DNA interacting with increasing concentrations of the compound (12.5–50  $\mu\text{M}$ ); lane 5, EcoRI-treated pUC18 plasmid DNA in 0.1% DMSO; lanes 6–8, EcoRI-treated pUC18 plasmid DNA interacting with increasing concentrations of the compound (from 12.5 to 50  $\mu\text{M}$ ). Gels at the C line: lane 1, HindIII-treated pUC18 plasmid DNA in 0.1% DMSO; lanes 2–4, HindIII-treated pUC18 plasmid DNA interacting with increasing concentrations of the compound (12.5–50  $\mu\text{M}$ ).